Title
The Role and Mechanism of Meiotic Chromosome Motion in C. elegans

Author
Wynne, David

Publication Date
2010

Peer reviewed|Thesis/dissertation

The Role and Mechanism of Meiotic Chromosome Motion in *C. elegans*

By

David J. Wynne

A dissertation submitted in partial satisfaction of the

requirements for the degree of

Doctor of Philosophy

in

Molecular and Cell Biology

in the

Graduate Division

of the

University of California, Berkeley

Committee in Charge:

Professor Abby F. Dernburg, Chair
Professor W. Zacheus Cande
Professor Rebecca Heald
Professor Sanjay Kumar

Spring 2010

Abstract

The Role and Mechanism of
Meiotic Chromosome Motion in *C. elegans*

by

David J. Wynne

Doctor of Philosophy in Molecular and Cell Biology

University of California, Berkeley

Professor Abby F. Dernburg, Chair

Proper meiotic chromosome segregation in *C. elegans* requires homolog pairing, synapsis, and recombination. The mechanisms underlying homologous chromosome pairing remain poorly understood. In *C. elegans*, as in many other eukaryotes, pairing is accompanied by a global rearrangement of chromosomes. Work from the Dernburg lab and others has found that this rearrangement is driven through the association of special chromosome regions known as Pairing Centers (PCs) with nuclear envelope proteins and cytoskeletal components (Phillips et al. 2005, Sato et al. 2009). Using fluorescent markers for nuclear envelope attachment sites and Pairing Centers, I analyzed prophase chromosome dynamics through real-time imaging and quantitative motion tracking. My results reveal a dramatic increase in chromosome motion at the onset of chromosome pairing that persists after homologous loci are paired. I show that this increased mobility correlates with the formation of NE patches, and that the increase in motion that accompanies meiotic entry is abrogated by knockdown of cytoplasmic dynein. These rapid motions are also sensitive to depolymerization of microtubules by colchicine, but are not affected by treatment with Latrunculin A. In addition, fluorescent labeling of whole chromosomes suggests that meiotic chromosome motion is driven primarily by the PC end of chromosomes and that the chromosome is quite flexible. These data support a model in which meiotic chromosome motion is promoted by a small number of fast, microtubule-dependent, motor-driven movements that augment the smaller, likely diffusive motions seen prior to meiosis. The observation that fast motions persist well after pairing is completed suggests additional roles in chromosome synapsis or recombination, and are consistent with the idea that rapid motions function to destabilize inappropriate, non-homologous interactions.

Table of contents

List of Figures and Tables

Introduction

Homolog pairing and synapsis play essential roles in meiotic chromosome segregation

Meiosis, the specialized cell division that produces gametes, achieves a reduction in chromosome number by partitioning homologous chromosomes to different daughter cells. Faithful segregation of chromosomes is essential, since aneuploidy is usually lethal to the progeny. In some cases, meiotic errors result in developmental disorders like Down syndrome (trisomy 21) or Turner Syndrome (*X* monosomy) in humans. To ensure proper segregation during meiosis, a highly regulated series of interdependent steps takes place during meiotic prophase. Among the earliest of these is the formation of pairwise interactions between homologous chromosomes. This homologous pairing is then stabilized by synapsis, defined as the formation of the synaptonemal complex. This complex persists until late prophase, and is disassembled during diplotene-diakinesis to allow homologs to segregate during the first division. Proper pairing and synapsis are required in many organisms for crossover recombination, which creates linkages between homologous chromosomes that enable them to biorient on the metaphase pate. Failure of homolog pairing, synapsis, or recombination typically results in inviable progeny, or to sterility as a consequence of checkpoints that arrest meiotic progression prior to fertilization. The mechanisms that facilitate homolog pairing and enable chromosomes to properly "recognize" homology remain among the most mysterious aspects of meiosis. My work has used *in vivo* imaging of meiotic chromosomes during early prophase to address these important questions in *C. elegans.*

Pairing and the transition to synapsis

The synaptonemal complex (SC) is a tripartite structure consisting of axial elements that form linear cores or axes along each chromosome and central elements that normally polymerize between the axes of homologous chromosomes, holding them together like a zipper. Hereafter, I will use the term synapsis to describe the polymerization of the central elements along the chromosome axis. The sites of synapsis initiation vary among organisms and the mechanisms that determine these sites are not well understood. Genetic analysis in multiple systems has revealed that synapsis can occur independently of homology. Mutants exist in *S. cerevisiae*, maize, and *C. elegans* in which synapsis occurs between inappropriate partners including nonhomologous chromosomes, folded-over regions of a single chromosome, and between a single chromosome and multiple partners (Golubovskaya et al., 2002; Leu et al., 1998; Martinez-Perez and Villeneuve, 2005). There is also evidence from *S. cerevisiae* showing that the central element protein Zip1 can polymerize between non-homologous centromeres in a normal meiosis (Tsubouchi and Roeder, 2005). Taken together, these data raise the possibility that synapsis may be largely independent of homology even in wildtype cells and that barriers to non-homologous synapsis exist that help coordinate synapsis initiation with correct pairing.

One way to address what mechanisms are employed to transition from correct pairing to synapsis is to look at where synapsis initiates in normal meiosis. Cytologically, small stretches of central elements have been observed both near chromosome ends

and at multiple sites along chromosomes. Since synapsis is thought to be quite processive these short stretches have been interpreted as central elements soon after synapsis initiation. In *S. cerevisiae*, where this has been extensively studied, synapsis is thought to initiate in primarily at sites of crossover recombination. In the absence of recombination in *S. cerevisiae*, normal synapsis does not occur. Similar results have been observed in other model systems, including mice and plants (Giroux et al., 1989; Romanienko and Camerini-Otero, 2000). Further, a protein complex known as the Synapsis Initiation Complex (SIC) that is required both for recombination and normal synapsis in *S. cerevisiae* has been shown to localize to discrete foci on meiotic chromosomes whose spacing mirrors the nonrandom distribution of crossovers caused by interference (Fung et al., 2004). In stark contrast to the situation in *S. cerevisiae*, synapsis appears to begin exclusively at sites called Pairing Centers (PCs) in *C. elegans* (discussed further below) and does not require recombination. Loss of the endonuclease *spo-11* that generates meiotic double strand breaks required for recombination has no apparent effect on synapsis in *C. elegans* (Dernburg et al., 1998). Cytological analysis of translocation heterozygotes in *C. elegans* shows that the presence of homologous PCs is sufficient to cause synapsis through large regions of non-homologous sequence, which suggests that once initiated, synapsis proceeds along the entire chromosome axis from the PC region (MacQueen et al., 2005).

Despite the apparent differences between synapsis initiation in *S. cerevisiae* and *C. elegans*, recent work in both systems has suggested that similar molecular mechanisms may contribute to synapsis in both organisms. In *S. cerevisiae*, stretches of central elements have been observed near nonhomologously paired centromeres in the absence of recombination, and two proteins that appear to restrict synapsis initiation at centromeres were recently identified (Macqueen and Roeder, 2009; Tsubouchi and Roeder, 2005). Conversely, in *C. elegans* a mutant has been found (*cra-1*) in which central elements polymerize non-homologously and this polymerization requires the *C. elegans* homologs of MSH5, RAD51, MRE11, and SPO-11, proteins that are required for recombination and/or double strand break formation (Smolikov et al., 2008). The aberrant synapsis seen in *cra-1* therefore depends on intermediates along the pathway to recombination. These mutant situations in budding yeast and worms suggest that if you impair the mechanisms of synapsis initiation that normally dominate you reveal polymerization of central elements that initiate by mechanisms that are dominant in other organisms, i.e. you reveal recombination-intermediate-dependent central element polymerization in worms and central element polymerization at pairing sites in *S. cerevisiae*. One interpretation of these results is that stabilization of pairing, regardless of how it is achieved, has the potential to initiate central element polymerization in both systems. In plants and mammals, where synapsis is thought to initiate both at telomeres and at interstitial loci, this may reflect stabilization of pairing through simultaneous processes of alignment in the bouquet and recombination, respectively (Corredor et al., 2007; Pfeifer et al., 2003).

Alternatively, the barrier to synapsis may be overcome by other mechanisms that are satisfied by pairing site interactions or recombination, such as changes in chromatin structure or modification of SC components. In *S. cerevisiae*, modification by the ubiquitin-like molecule SUMO has been shown to be required for efficient synapsis and there is evidence that the central element binds preferentially to axial element proteins

that have been conjugated to SUMO, providing a possible mechanism governing synapsis (Cheng et al., 2006; Hooker and Roeder, 2006). Mutation of the single gene encoding SUMO in *C. elegans* (*smo-1*) does not appear to affect SC formation, indicating that any function in synapsis in *C. elegans* is not essential. However, it remains possible that *smo-1* mutants are not truly null for SUMO function, perhaps due to persistence of maternal product deposited in the egg (Bhalla et al., 2008).

It remains to been seen whether a universal mechanism linking stable pairing to synapsis exists. Until synapsis initiation and the barrier to non-homologous synapsis are understood more completely in any one organism it will not be possible to address the conservation of these processes.

Special chromosomal loci contribute to homolog pairing and synapsis in different organisms

A major unresolved question is what function special chromosome sites play in the processes of pairing and synapsis. Evidence from diverse model systems has shown that specific chromosomal loci act in *cis* to promote pairing and/or synapsis. Understanding the function of these loci is essential for an understanding of pairing and synapsis and these sites have provided powerful tools to investigating meiotic chromosome dynamics. Genetic studies in maize (*Zea Maize*), *Drosophila* (*Drosophila melanogaster*) and *Caenorhabditis elegans* used various chromosomal rearrangements such as translocations and deletions to show that some genomic locations have drastically different effects on recombination. These observations led to models in which the differences in recombination resulted from specific loci being particularly effective in pairing (Hawley, 1980; Maguire, 1986; McKim et al., 1988; Villeneuve, 1994). A *cis*-acting site in the rDNA of the *Drosophila* sex chromosomes was also found to be required for X-Y segregation in *Drosophila* males, which undergo an unusual meiotic program that lacks both synapsis and recombination (McKee et al., 1992; McKee and Karpen, 1990). In *Drosophila* female meiosis and maize, it remains unclear how the potential pairing sites may mediate homologous interactions. In *C. elegans,* cytological analysis has provided direct evidence that pairing sites, known as a Homolog Recognition Regions or Pairing Centers (PCs), mediate homologous pairing (MacQueen et al., 2005). Further work has shown that PCs promote pairing by recruiting a family of zinc finger proteins. If these PC-binding proteins are disrupted by mutation, no pairing occurs at the PC (Phillips and Dernburg, 2006; Phillips et al., 2005). *Trans*-acting factors were also found to be required for the function of the X-Y pairing site in *Drosophila* males. The Stromalin in Meiosis (SNM) and Modifier of Mdg4 in Meiosis (MNM) proteins both localize to these pairing sites and are required for X-Y pairing (Soltani-Bejnood et al., 2007; Thomas et al., 2005). Interestingly, a third protein called teflon is required for pairing of the autosomes in *Drosophila* males . Like the PC-binding proteins in *C. elegans*, it also contains C2H2 Zn-finger domains (Arya et al., 2006; Tomkiel et al., 2001). The Teflon protein has been proposed to mediate interaction between heterochromatic regions rather than at specific pairing sites so it is not yet clear that there is any mechanistic similarity between the function of pairing sites in *C. elegans* and *Drosophila* males.

The extent to which centromeres act as meiotic pairing sites is still unclear. Homologous centromeres have been shown to associate more often than other

homologous loci in meiosis in fission yeasts (*S. pombe)*, budding yeast (*S. cerevisiae*), and wheat (Ding et al., 2004; Martinez-Perez et al., 2001; Scherthan et al., 1994; Tsubouchi and Roeder, 2005). In *Drosophila,* the pericentric heterochromatin is paired in meiotic prophase and homology in this region has been sown to be required for the segregation of homologous chromosomes that fail to undergo recombination (Dernburg et al., 1996; Karpen et al., 1996). However, centromeres have not been causally linked to the establishment of homolog pairing or the progression to stabilization of pairing in normal meioses in any system. Centromere associations in meiosis have also been shown to include heterologous as well as homologous interactions, and centromeres also associate in non-meiotic cells (Fransz et al., 2002; Jin et al., 1998; Scherthan et al., 1994). Thus, it is possible that the interactions between centromeres in meiosis represents transient interactions that contribute little to meiotic pairing and may even inhibit pairing by other, more robust pairing mechanisms.

Telomeres, Nuclear Envelope attachment, and the meiotic bouquet may all contribute to homolog pairing and synapsis

A second major question is the role of meiosis specific chromosome dynamics in the processes of pairing and synapsis. Telomeres play a well established role in meiosis by attaching to the nuclear envelope and clustering together to generate a polarized chromosome arrangement called the bouquet conformation (reviewed by Scherthan, 2001). This dramatic reorganization of chromosomes has been known since the beginning of the twentieth century when the bouquet confirmation was named because the telomere-proximal regions of chromosomes were reminiscent of parallel flower stems clustered in a vase. This meiotic nuclear architecture is widely conserved and has been shown in multiple systems to be coincident with homologous pairing and the initiation of synapsis (Bass et al., 2000; Scherthan et al., 1996; Vazquez et al., 2002). However, the mechanisms by which the bouquet confirmation plays a causal role in pairing and synapsis remain unclear. Telomeres do not seem to act as pairing sites *per se* because there is little evidence that homologous telomeres interact more than heterologous telomeres. One leading model is that the clustering of telomeres helps align chromosomes and thereby increase the proximity of homologous loci because they lie at the same distance from the telomere. However, this mechanism may not be universal because non-typical bouquet conformations, in which either the telomeres are only loosely clustered or not clustered at all, have been observed in multiple systems. Another proposed function for the bouquet conformation is to eliminate topological entanglements like interlocks, in which one or more chromosome axis is caught between two chromosomes as they pair and synapse. Interlocks pose a major barrier to complete alignment, particularly in organisms with a large genome size, like maize, which has been shown to have a high frequency of interlocked chromosomes at the beginning of pachytene (Wang et al., 2009). Some mutations that disrupt normal bouquet formation also have an increased number of interlocks and it has been proposed that there are mechanisms that actively resolve interlocks during the time that chromosomes are in the bouquet (Golubovskaya et al., 2002; Koszul et al., 2008; Storlazzi et al., 2010). Although the bouquet conformation has been recognized since the beginning of the twentieth century as a broadly conserved feature of early meiotic prophase, the mechanisms by which it contributes to homolog pairing and

stabilization of pairing remain poorly understood (reviewed by Scherthan, 2001; Zickler and Kleckner, 1998).

In recent years it has become clear that the transmembrane NE proteins involved in chromosome attachment at the bouquet stage are also well conserved. Pairs of transmembrane inner and outer NE proteins contain SUN and KASH domains, respectively, and bind to one another in the lumenal space forming a bridge from the nucleoplasm to the cytoplasm. KASH domains (named for *K*larsicht/*A*NC-1/*S*yne/*h*omology) are thought to interact with SUN (named for *S*ad1/*UN*C-84) domain-containing binding partners to connect various cytoskeletal components to the nucleus (reviewed by Starr and Fischer, 2005). SUN domain proteins usually have a single transmembrane domain and localize within the inner nuclear membrane (INM) with their SUN domain oriented into the lumen of the NE (Hiraoka and Dernburg, 2009; Malone et al., 1999). Functional evidence that pairs of SUN/KASH proteins play a role in chromosome attachment to the NE in meiosis exists in *S. pombe*, and *C. elegans* and SUN domain proteins that play a role in telomere attachment are known for *S. cerevisiae* and mice but their outer NE partners are either unknown or do not share obvious homology with other KASH domains (Conrad et al., 2007; Ding et al., 2007; Lei et al., 2009; Penkner et al., 2007; Sato et al., 2009). SUN/KASH pairs play a variety of roles outside of meiosis in connecting NE components to cytoskeletal components (reviewed by Starr and Fischer, 2005).

Inside the nucleus, the components that mediate chromosome attachment to the NE in meiosis are much more divergent among species. In *S. pombe*, the telomere binding proteins Rap1p and Taz1p, the meiosis-specific proteins Bqt1p and Bqt2p, and the ubiquitously-expressed Bqt3p and Bqt4p are all required for proper bouquet formation (Chikashige et al., 2006; Chikashige et al., 2009; Cooper et al., 1998; Nimmo et al., 1998; Tang et al., 2006). In *S. cerevisiae*, the novel protein Ndj1p binds to telomeres and attaches chromosomes to the SUN protein Mps3p (Chua and Roeder, 1997; Conrad et al., 1997; Conrad et al., 2007). Meiotic chromosome/NE attachment in *C. elegans* has one intriguingly divergent feature in that the PC of each chromosome is tethered to the SUN/KASH complex rather than the telomeres (Sato et al., 2009). In *C. elegans,* only a single end of each chromosome had been shown to attach to the NE by electron microscopy and this data fit well with the discovery of the involvement of PCs in meiosis, which are each located near the end of a chromosome (Goldstein and Slaton, 1982). Further, the PCs in *C. elegans* do not cluster as telomeres do in a canonical bouquet conformation but a dramatic rearrangement of chromosome morphology still occurs and there is correlative evidence that this rearrangement plays a role in promoting pairing (MacQueen and Villeneuve, 2001). Thus, the *C. elegans* pseudo-bouquet highlights the possibility that chromosome tethering to SUN/KASH complexes promotes pairing without contributing to alignment as in other systems.

Meiotic prophase chromosome motions: a minireview of live imaging studies

A handful of recent studies have begun to shed light on a new feature of meiotic chromosome dynamics that is likely to play an important role in the processes of pairing and synapsis. Rapid chromosomal motions have been observed in multiple systems and are now emerging as a well conserved feature of meiotic prophase. The earliest study documenting this behavior was done in cultured rat spermatocytes. Parvinen and

Soderstrom used a new protocol to extract living, staged rat spermatocytes to verify that meiotic chromosome motions, which had been observed previously, occurred specifically at the time of pairing and synapsis (during the meiotic stages of leptotene and zygotene). They reported that motions begin during leptotene, reach their peak during early zygotene, and then decrease until motion is rare during early pachytene, the meiotic stage in which synapsis has been completed, and non-existent by mid-pachytene. They went on to analyze this motion by tracing chromosomes at 15s intervals and show that chromosomal rotations vary in degree and direction, appearing random (Parvinen and Soderstrom, 1976). In the years since that work, little progress was made addressing the function of these motions until microscopy and fluorescent labeling methods improved substantially. Rapid chromosomal motions have now been recorded during live meiosis in *S. pombe*, *S. cerevisiae*, and maize (Chikashige et al., 1994; Conrad et al., 2008; Ding et al., 1998; Ding et al., 2004; Koszul et al., 2008; Scherthan et al., 2007; Sheehan and Pawlowski, 2009; Trelles-Sticken et al., 2005), and longer-term motions have been recorded in cultured mouse spermatocytes (Morelli et al., 2008). Some of the most detailed work comes from studies in *S. pombe*, and has revealed that the entire nucleus migrates back and forth throughout the length of the cell during virtually the entire period between karyogamy (fusion of the haploid nuclei) and segregation of chromosome at metaphase of meiosis I (Chikashige et al., 1994). Further studies of this "horsetail stage," as it became known, revealed that the motion is dynein- and MT-dependent and that it requires telomere attachment to the spindle pole body (SPB), the fungal MT-organizing center (Ding et al., 1998; Ding et al., 2004; Miki et al., 2002). The current model for the mechanism driving horsetail motion is that MT filaments grow out from the SPB and interactions between MTs, and both MT-bound, and cortical dynein pull the SPB in the direction of the longest MTs. When the ends of the leading MTs reach the cortex, the leading filaments shorten and the SPB changes direction to follow growing MTs on the opposite side (Chikashige et al., 2007; Vogel et al., 2009).

One particularly interesting study of horsetail motion looked at the behavior of multiple loci along chromosomes. Ding et al. used LacO insertions and GFP-LacI to mark specific loci for live analysis. They were able to show that the distance between homologous loci fluctuates over the course of the horsetail stage, with the average distance decreasing progressively over time. This progressive pairing is dependent on nuclear oscillation and the tethering of telomeres to the SPB, and it also depends on recombination. This is consistent with other data that indicates that crossover formation is the primary mechanism that stabilizes pairing in *S. pombe,* which lacks a classical SC. Because the horsetail nuclear oscillations are thus far unique to *S. pombe*, it is not clear which aspects of this analysis can be extrapolated to other organisms. Important differences from the rapid prophase movements described here and in other studies are that the movement of the entire nucleus during the horsetail stage in *S. pombe* is relatively slow (5 μm/minute), and the telomeres maintain a very tight association with the SPB and do not show independent movements, as they do in budding yeast, and as we have observed for Pairing Centers in *C. elegans*.

The only other system in which meiotic chromosome motion has been analyzed by multiple groups is *S. cerevisiae.* Trelles-Sticken et al. used live imaging of telomere reporters to show that telomeres cluster only temporarily in zygotene, providing direct

evidence for a bouquet stage in *S. cerevisiae*, which had been controversial since telomere clustering is never tight. They went on to show that formation of this bouquet is actin-dependent, and its dispersal requires the cohesin subunit protein Rec8 (Trelles-Sticken et al., 2005). Scherthan et al. extended this work using a fluorescent reporter for the central element protein Zip1p to label the entire length of meiotic chromosomes. These authors showed that chromosome motions were accompanied by deformations of the nuclear envelope, again in an actin-dependent manner that requires attachment of telomeres to the nuclear periphery (Scherthan et al., 2007). More recently, two groups extended this analysis further. Conrad et al. used a new 3D imaging approach to image Rap-1-labeled telomeres. They quantified the motion they observed and classified rapid prophase motions (RPMs) as a unique class that can exceed 1 um/s, require nuclear attachment, and begin prior to pachytene but persist throughout pachytene (Conrad et al., 2008). Koszul et al. used a combination of telomere, central element, NE, and actin reporters to visualize chromosome motion in pachytene. They presented a model in which telomeres drive chromosome motion by attachment to actin filaments that surround the outside of the nuclear envelope. They further suggested that the transient telomere clustering that has been interpreted as a loose bouquet in *S. cerevisiae* is an indirect result of a tendency of actin filaments to cluster in the vicinity of the SPB (Koszul et al., 2008).

In light of this evidence that the prophase movement of chromosomes in *S. pombe* and *S. cerevisiae* are not only qualitatively and quantitatively different, but also occur by distinct molecular mechanisms, studies in other organisms will help to assess the conservation of these processes and to address their function in meiosis. This has been challenging, particularly in multicellular organisms where the reproductive tissues may not be amenable to cytological analysis. Sheehan and Pawlowski overcome this by using two-photon microscopy to analyze cultures of intact anthers from maize following vital staining of the DNA (Sheehan and Pawlowski, 2009). They describe multiple classes of chromosome motion, including rotation of the entire chromosome mass, and fast motions of single chromosome segments similar in speed to those seen in *S. cerevisiae* (ave. speed of 0.4 μm/s in zygotene). These motions appear to share other similarities with *S. cerevisiae,* including being telomere-led and coupled with deformation of the NE. However, fast motions in *S. cerevisiae* persist throughout the pachytene stage, while motion in maize slows in pachytene (to an average speed of ~0.15 μm/s). In addition, motions in maize are sensitive both to actin and MT-depolymerizing drugs, so the cytoskeletal contribution is somewhat unclear.

An additional study examined spermatocytes dissected from mice expressing fluorescent central element proteins (Morelli et al., 2008). This work corroborated the observations of Parvinen and Soderstrom, and found that prophase motions are slower than those recorded in *S cerevisiae.* However, the conclusions of this study are subject to the caveat that the spermatocytes were removed from their natural environment to allow imaging.

Taken together, these studies suggest that some features of early prophase motions are broadly conserved. Major unresolved questions include whether meiotic chromosome motion is driven by the actin or microtubule cytoskeleton, and how it contributes to pairing, synapsis, and other meiotic processes.

Concluding Remarks

The work presented here contributes to our understanding of pairing and synapsis by extending the live analysis of early prophase chromosome dynamics to *C. elegans*. This work provides the first observations of meiotic chromosome dynamics in a live animal. Using these observations, I address whether rapid chromosome motions are conserved in *C. elegans* and investigate the role of the cytoskeleton in these dynamics. I investigate the effects of rapid meiotic motions on chromosome pairing at Pairing Center loci and use these data to argue that the role of rapid motions is not limited to promoting association between homologous chromosomes but may actually oppose pairing and provide stringency to the pairing process that prevents the stabilization of non-homologous pairing.

Chapter I: Chromosomes Exhibit Rapid Motion During Early Meiotic Prophase in *C. elegans* that Is Unlikely to Be a Result of Diffusion

Summary

This chapter describes the characterization of chromosome motions in early meiotic prophase in *C. elegans*. The nuclear envelope protein, ZYG-12, forms cytologically distinct aggregates in early meiotic prophase that mark the sites of chromosome attachment to the nuclear envelope and can thereby serve as a reporter for chromosome dynamics. I present high-speed, high-resolution, time-lapse, microscopy used to visualize fluorescently-labeled ZYG-12 dynamics during early meiotic prophase in intact animals. I analyze the biophysical properties of this motion using quantitative motion tracking and show that chromosome behavior is not likely to be the result of diffusion. This work marks the first characterization of early prophase chromosome motion in a living animal system.

Introduction

As discussed above, there is substantial evidence that meiotic chromosome pairing and synapsis involves a number of features including the activity of special pairing loci, chromosome attachment to the NE, the polarized meiotic bouquet chromosome conformation, and newly-discovered rapid chromosome motions. However, the mechanisms by which chromosome dynamics contribute to pairing and synapsis remains unclear. Moreover, variations of the bouquet and rapid prophase movements that have been observed in various organisms have made the underlying similarities in these processes, if any exist, hard to determine. Thus, an essential next step is to extend our investigation of meiotic chromosome dynamics to new organisms.

C. elegans has emerged as a powerful model system in which study meiosis and many conserved as well as novel meiotic components have been characterized. Work in *C. elegans* has shed light on components required for chromosome pairing. Specialized sites known as Homolog Recognition Regions or Pairing Centers (PCs) are present on each worm chromosome and are required in *cis* for pairing and efficient synapsis of their cognate chromosome (MacQueen et al., 2005; McKim et al., 1988; Villeneuve, 1994). An important breakthrough in understanding the function of these loci came from analysis of the gene *him-8*, which had long been known to be important for segregation of the X chromosome in *C. elegans.* In *C. elegans,* sex is determined by the number of X chromosomes with the XX genotype specifying the hermaphrodite fate and hemizygous XO animals developing as males. In normal lab strains, the progeny of self-fertilizing hermaphrodites are virtually all hermaphrodites (> 99%) while males arise through occasional nondisjunction of the X chromosome. Due to this, a high frequency of males in a population reflects chromosome segregation defects, an observation that served as the basis for multiple genetic screens that identified mutants with a *h*igh *i*ncidence of *m*ale progeny, or “Him” phenotype, of which *him-8* was one (Hodgkin et al., 1979). The convergence between *him-8* and PC function occurred much more recently through genetic analysis showing that loss of *him-8* function enhanced the number of male progeny produced by animals that were heterozygous for a deficiency of the X chromosome pairing center, suggesting that *him-8* functioned along with the X PC to promote accurate segregation of the X chromosome (Phillips et al., 2005). Cytological analysis of the HIM-8 protein revealed that it localized specifically to the *X* chromosome and that mutations in *him-8* cause loss of pairing and synapsis of only the *X* chromosomes, phenocopying the effect of loss of the X PC. In subsequent work it was found that *him-8* lies in an operon encoding three other paralogous Zn-finger proteins (named *zim-1*, *zim-2* and *zim-3* for ‘*z*inc finger *i*n *m*eiosis’) that localize to the PCs of the autosomes and are required for pairing and synapsis of specific chromosomes (Phillips and Dernburg, 2006). These PC-binding proteins are the first *trans*-acting factors identified in any system that are required for pairing and synapsis in a chromosome-specific manner.

Another finding that contributed to understanding the function of the PCs was the observation that PCs, along with their cognate HIM-8 and ZIM proteins, localize to the NE during the transition zone region of the gonad, which corresponds to the leptotene/ zygotene stages of meiotic prophase. This localization was exciting because it was reminiscent of telomere attachment to the NE, which plays a well established role in

meiosis in other systems. That similarity was borne out when the NE protein ZYG-12 was found to aggregate into cytologically distinct patches in the transition zone that perfectly colocalize with HIM-8 and ZIM proteins (Sato et al., 2009). ZYG-12 had been previously identified in *C. elegans* as a HOOK protein required for attachment between the nucleus and centrosome (Malone et al., 2003). HOOK proteins contain an N-terminal domain that interacts with microtubules (MT), a central coiled coil domain, and a divergent C-terminus and are thought to connect organelles to MTs (Walenta et al., 2001). The C-terminus of ZYG-12 contains a small KASH domain and ZYG-12 requires SUN-1 for localization to the NE. SUN-1 turned out to reside in and be required for the formation of the cytological foci in the transition zone that colocalize with PCs (Penkner et al., 2007). The topological organization and binding between ZYG-12 and SUN-1 have also now been tested directly in *C. elegans,* validating them as a true SUN/KASH pair (Minn et al., 2009). The identification of a SUN domain protein that interacts with PCs in *C. elegans* proved the similarity to telomere attachment in other systems. The characterization of SUN-1 and ZYG-12 in *C. elegans* meiosis helped place what was known about PCs into the larger context of the meiotic bouquet formation or, more generally, chromosomal reorganization during pairing and synapsis.

Having established that PCs are interacting with protein complexes that are conserved in meiosis, it follows that the mechanisms by which PCs are promoting pairing and synapsis are also conserved. A major question then is whether or not PCs exhibit the rapid chromosome motions in early prophase that have been seen in other organisms. If rapid motions exist, *C. elegans* can provide and excellent tool to investigate their function. *C. elegans* is an excellent system in which to investigate pairing and synapsis because it allows us to visualize early meiotic chromosome dynamics *in situ* in living animals. Adult worms contain 300-500 meiotic nuclei arranged in temporal order that can be imaged through the worm's transparent tissues without dissection. To date, studies of meiosis in *C. elegans* have taken advantage of the gonad architecture but have been restricted to analysis of fixed specimens that permit only a steady-state picture of dynamic processes. *In vivo* imaging is required to understand pairing associations both because it allows one to directly visualize time progression in a single nucleus and because it is able to capture transient events that would be missed in static images. Precise measurement of chromosome motion is necessary to understand the mechanisms that generate motion and to understand how motion contributes to pairing and synapsis. If motions exist in *C. elegans*, it will be important to determine if they are driven by molecular motors, as has been seen in other organisms or if PC loci can mediate pairing and synapsis by relying on diffusive motion alone. In Chapter I, I present a detailed analysis of chromosome dynamics based on high-speed, high-resolution time-lapse imaging. I verify that PC attachment sites are extremely dynamic both in speed and overall number and present quantitative analysis that suggests this motion is driven by active forces.

Results

Patches of Nuclear Envelope proteins that mark Pairing Center attachment sites are extremely dynamic

To investigate the dynamics of NE patches in live animals I took advantage of a strain made previously that expresses ZYG-12::GFP in the gonad. This reporter proved extremely well-suited to live imaging due to its brightness. The robustness of the ZYG-12::GFP fluorescence made it possible to subject animals to many exposures without losing the signal due to photobleaching. Live imaging revealed that ZYG-12 patches are extremely dynamic (Figure 1). Because ZYG-12 patches move all around the nuclear envelope imaging a single plane only allows capture of a small percentage of ZYG-12 motions (Figures 1C-D). 3D imaging is required to visualize all ZYG-12 motion in a nucleus. The brightness of the ZYG-12::GFP reporter made it possible for it to be visualized using the high speed imaging capabilities of the OMX imaging system in collaboration with Pete Carlton who moved to John Sedat's lab at UCSF (Carlton et al., in preparation). Imaging ZYG-12::GFP using the OMX allowed us to collect 25 or more optical sections with .25 μm spacing at 2 Hz, which covered a large enough distance in Z (6 μm) to capture the full volume of most nuclei in a field (Figure 2).

It was clear from prior work using static images that the number of NE patches present in each nucleus in the transition zone varies (Penkner et al., 2007; Sato et al., 2009) and (Figure 2A). Live analysis revealed that the number of NE patches on the surface of a single nucleus is extremely dynamic. Patches can be seen merging and splitting often in 2 min time-courses. An example nucleus in which two patches merge, remain together for at least 12 s (4 time points), and split apart again can be seen in Figures 2B-D. To quantify the mobility of patches I selected nuclei of which the complete volume was visible for the entire dataset and tracked all patches throughout the 2 min data collections. Since the identity of a patch cannot be followed unambiguously beyond merging with another patch I generated trajectories according to the following three rules. First, multiple patches were only assigned to a single ZYG-12 focus if they merged into a single focus from multiple foci in an earlier time point or split into multiple foci in a subsequent time point. Second, patches were only tracked if they remained present as an individual for 10 time points (≥ 20 s). Third, when the connectivity between patches was ambiguous from time point to time point (typically because two patches were assigned to a single focus or two patches of similar size and brightness remain close together in successive time points) I favored connections that produced the least motion. Following these rules, I could most often generate trajectories that follow 6 patches in a nucleus and I could describe almost all nuclei (24/26) with 4-6 patches (Figure 3A-C). Since we know from previous work that all ZYG-12 patches are occupied by at least one PC, this result suggests that most of the patches correspond to two chromosomes, most likely two homologous paired PCs, and, surprisingly, that some patches represent more than 2 chromosomes. Since there are 4 PC-binding proteins (HIM-8, ZIM-1, ZIM-2, and ZIM-3) and 6 pairs of homologous chromosomes, a likely explanation for this result is that ZIM-1 and ZIM-3, the two PC-binding proteins that bind to multiple chromosomes, often form a single patch that aggregates the PCs of four chromosomes.

NE patch dynamics are unlikely to be the result of diffusion

During the majority of time points, ZYG-12 patch speeds were below 0.2 μm/s but there were occasional time points that catch much faster motions from ~0.4-0.6 μm/s. A representative nucleus is shown in Figures 3A and 3B in which all but one of the patches undergoes at least one jump around 0.4 um/s or above during the 2 min. time-course. When the data for all ZYG-12 patches are analyzed together (n = 133 patches from 26 nuclei in 3 gonads) the mean speed is 0.124 ± 0.101 μm/s and the mean of the top 5% of all speeds captured was 0.434 ± 0.093 μm/s. Thus, the top 5% of speeds seems to be a good representation of these rare, fast motions.

Because of the occasional spikes in the speed of ZYG-12 patch motion, it seemed unlikely that the mobility of ZYG-12 was the result of a diffusion-based process. Diffusion alone should result in much more uniform speeds. As a formal test of this idea, I compared the distribution of step sizes for ZYG-12 motion to a normal distribution, which would be expected for diffusion-based motion (Berg, 1993). I compiled all the individual displacements in X, Y, and Z for adjacent time points, which generated a curve centered at 0 (Figure 4C). Next, I found the normal distribution that best fit this distribution of ZYG-12 step sizes by generating normal distributions with a wide range of standard deviations (.05 - 0.4μm) and computing the differences between each of these distributions and the ZYG-12 data. The result was that a normal distribution with a standard deviation of 0.15 μm best fit the ZYG-12 step sizes (Figure 4C, yellow curve) but showed significant deviations from the ZYG-12 distribution. In contrast, since I had seen an infrequent number of much faster motions, I wondered if the ZYG-12 data could be better fit by using a combination of two normal distributions, presuming that a second distribution could take into account these faster motions. To do this, I expanded the best-fit algorithm to generate a series of distributions that each represent the sum of two normal distributions, sampling a wide variety of standard deviations for each and combining the two at a range of ratios from 1:0 to 1:1. Interestingly, The best fit curve produced using this method (Figure 4C, purple), which was the sum of normal distributions with standard deviations of 0.01 μm and 0.35 μm combined in a ratio of 3:1 (Figure 4C, red curves) fit the ZYG-12 data better than any single normal distribution. The fact that the ZYG-12 step sizes are not well represented by a normal distribution and that the data are better fit by a model combining two normal distributions support the notion that ZYG-12 motion is not the result of simple diffusion. Instead, diffusion-based motion may be present along with an additional source of motion, perhaps driven by molecular motors.

Chapter II: *X* Chromosomes Exhibit a Class of Rapid, Meiosis-Specific Chromosome Motions that May Function to Test Pairing of the PCs

Summary

In this chapter I present the development and characterization of fluorescent reporters that mark specific loci during meiosis in *C. elegans*. Analysis of chromosome motion using these reporters alone and in combination with methods to label whole chromosomes reveal that there is a class of rapid, end-directed chromosomal motions that are specific to nuclei that have entered meiosis. These rapid motions persist after pairing at the PC has been achieved and also persist, to a lesser degree, after chromosomes have synapsed. Interestingly, analysis of X chromosome PC motion shows that PC regions can become unpaired after they have paired and, moreover that rapid motions do not tend to bring unpaired PCs closer together. These data do not support the idea that rapid motions promote pairing and, instead, suggest that rapid motion may play a role in opposing the stabilization of non-homologous interactions.

Introduction

Multiple models have been proposed for the function of rapid motions in meiotic prophase. These include bringing homologous chromosomes into proximity to promote pairing, moving chromosomes relative to one another to alleviate topological constraints such as interlocks that can serve as a barrier to stabilization of pairing, and providing a testing mechanism that opposes ectopic pairing events (reviewed by Koszul and Kleckner, 2009). Interestingly, in *C. elegans* loss of dynein and MTs in meiosis has a different consequences on homolog pairing and synapsis than loss of NE patch components. When MT are depolymerized with colchicine no pairing or synapsis is seen. In contrast, when dynein function is depleted through a combination of mutation and RNAi, there is a delay in pairing and a much stronger defect in synapsis. In addition, loss of the inner NE patch component, SUN-1, using a meiosis-specific hypomorphic allele, *sun-1(jf18)*, causes a loss of pairing but it also results in precocious synapsis between non-homologous chromosomes (Penkner et al., 2007; Sato et al., 2009). This surprising phenotype suggests that there is a barrier to precocious synapsis in wild-type animals that depends on *sun-1* function. Interestingly, Sato et al. showed that the defect in synapsis seen after dynein knockdown is lost when *sun-1* function is also reduced and that the synapsis that occurs is not limited to homologous chromosomes. This result led them to propose a new model in which dynein and *sun-1* play opposing roles on synapsis initiation, with dynein being required to overcome the barrier to precocious synapsis established by *sun-1*.

To fully understand how homologous pairing is achieved and coordinated with synapsis in *C. elegans* it is essential to establish in detail what chromosomal dynamics occur as chromosomes pair and synapse. My observations of ZYG-12 patch motion presented in Chapter I made it clear that the rapid prophase chromosome motions seen in other organisms are present in *C. elegans*. Analysis of ZYG-12 provided a detailed picture of PC motion but, because ZYG-12 labels the PCs of all chromosomes, and because it marks only the sites of chromosome attachment to the nuclear envelope, observations of ZYG-12 do not address motion along the rest of the chromosome or the relationships between motion and the processes of pairing and synapsis. Additional reporters are required to address these questions. In Chapter II, I present the development and characterization of a fluorescent reporter for the *X* Chromosome PC (X PC). I use this reporter to show that there is a dramatic increase in chromosome motion at the onset of meiotic prophase and to characterize a class of infrequent, rapid chromosome movements that augment the smaller, likely diffusion-based motions seen prior to meiosis. These motions are insensitive to the pairing of chromosomes and persist to a lesser degree after synapsis.

Combining the X PC reporter with fluorescent nucleotides that can be used to specifically mark the entire *X* Chromosome, I also show that chromosome motion occurs primarily at the PC end and that meiotic chromosomes appear quite flexible and elastic. In addition, the X PC reporter allowed me to make some observations about how motion relates to the process of pairing. I saw that unpaired X PCs do not gradually become closer together over the time-courses that I was able to image and I also found that rapid motions were as likely to move X PCs farther apart as they were to move them closer together. Surprisingly, I observed instances of X PCs coming

temporarily unpaired after pairing. Taken together, these data do not provide support for a model in which the function of rapid motions is to pair homologous chromosomes. Instead, these observations suggest that rapid motions can destabilize paired PCs, which may provide a barrier to the stabilization of pairing that could help restrict synapsis to correctly-paired PCs.

Results

Reporters for meiotic chromosome motion were generated using two complementary methods

In order to examine chromosomal motion in meiotic prophase I sought to mark both PC loci on specific chromosomes and components of the synaptonemal complex. In order to achieve stable expression of transgenes in the *C. elegans* germline constructs must be integrated into the genome in low copy number (Schaner and Kelly). I used two methods to achieve low copy integration of meiotic reporter constructs. By biolistic transformation (Praitis et al., 2001) I was able to generate a number of meiotic reporters using constructs driven by a variety of germline specific or meiosis specific promotors (Table 1). However, most of these were not well suited for live imaging because I could not detect fluorescence in live animals. One exception was a *gfp::him-8* construct driven with the *pie-1* promotor. This construct produced bright fluorescence but the strain had a high incidence of male progeny (Him) phenotype that is indicative of chromosome segregation defects in *C. elegans* (data not shown).

In parallel with biolistic transformation I also integrated reporter constructs using a method of homologous recombination coupled with transposon excision (Frokjaer-Jensen et al., 2008). I generated two strains with *gfp::him-8* driven by either the *htp-3* or *rad-51* promotors that had visible fluorescence in live animals (Figure 5A). The transgene driven by the *htp-3* promotor had brighter fluorescence so it was used for the remainder of this study. I verified the majority of the gene structure for the *htp-3p:gfp::him-8* construct using a series of PCR reactions (Figure 5B). The fusion protein expressed (hereafter GFP::HIM-8) formed distinct foci in germline nuclei in both the premeiotic and meiotic regions, recapitulating the localization of endogenous HIM-8 (Figure 6A). Next, I wanted to examine whether this fusion protein was functional and make sure that it did not interfere with normal chromosome pairing. To test this, I measured the frequency of male progeny, which would result from defects in X chromosome pairing (Figure 6B). This analysis showed that GFP::HIM-8 expression is not able to rescue a null mutation in *him*-8, however, it also shows that GFP::HIM-8 does not increase male production in a wildtype background, suggesting that it does not interfere with normal pairing. To confirm that GFP::HIM-8 expression does not interfere with normal pairing I measured *X* Chromosome pairing at the PC locus cytologically using immunofluorescence (Figure 6C). Quantification of pairing was done in animals expressing mCherry::Histone as well as GFP::HIM-8 because this strain was used for subsequent live imaging. These data confirm that expression of GFP::HIM-8 does not interfere with normal pairing and segregation of *X* Chromosomes and thus can be used as a reporter for normal chromosome behavior.

X Chromosome Pairing Center regions exhibit rapid motions that are specific to meiotic nuclei

Observation of GFP::HIM-8 in live animals revealed a dramatic increase in mobility of the *X* Chromosome PCs (X PCs) at the onset of meiotic prophase. Whereas each X PC in premeiotic nuclei remains largely restricted to a small region within the nucleus, X PCs in nuclei that have entered the transition zone move extensively around

the periphery of the nucleus (Figure 7). In order to quantify this behavior we collected high-resolution time-lapse datasets and tracked X PC motion in three dimensions.

Quantification verified the striking differences in motion presented in Figure 7. A plot of the mean squared displacements showed a dramatic increase in displacements for X PCs in the transition zone compared to those in premeiotic nuclei (Figure 8A). Plotting the distribution of speeds calculated for each individual step, corresponding to the distance travelled during the 5 s time intervals between data collection, revealed an intriguing difference (Figure 8B). The speeds for X PCs in premeiotic nuclei show a major peak at 0.030 μm/s and trail off with very few steps showing speeds above 0.100 μm/s. X PCs in transition zone nuclei show a much smaller peak around 0.030-0.040 μm/s and this peak trails off much more gradually, with many more speeds above 0.100 μm/s. With this in mind, I decided to analyze just the fastest speeds recorded for each class of PCs. Whereas X PCs in transition zone nuclei have only a slightly higher mean speed (0.082 ± 0.069 μm/s, n = 38 trajectories) than X PCs in premeiotic nuclei (0.039 ± 0.031 μm/s, n = 26 trajectories), comparison of the top 5% of speeds recorded for each class of nuclei (hereafter “mean maximum speeds”) shows that the mean maximum speeds increase dramatically for X PCs in transition zone nuclei to 0.291 ± 0.062 μm/s from 0.124 ± 0.064 μm in premeiotic nuclei (Figure 8C and D). These fast speeds make up only a small fraction of the total movements recorded in transition zone nuclei, with X PCs moving much like they do in the premeiotic region during many time points. Thus, a small number of infrequent, rapid motions appear to underlie the dramatic increases in mobility seen upon entry into meiosis.

The mobility of *X* Chromosome Pairing Centers does not change upon pairing

Having established that chromosome motion changes dramatically at the PC upon entering meiosis, I wondered if this behavior was specific for nuclei that have not yet paired with their appropriate homolog. To address this question, I compared the motion of X PCs in transition zone nuclei in which two GFP::HIM-8 foci were apparent, corresponding to unpaired *X* PCs, to the motion of PCs when only a single, bright GFP::HIM-8 focus appeared, corresponding to X PCs that have successfully paired. This comparison revealed strikingly similar motion in both classes (Figures 7 and 8). The mean squared displacement plots were virtually identical between these classes (Figure 8A) and the speed distributions were also similar, with both classes of nuclei showing many fast X PC motions above 0.100 μm/s (Figure 8B). Both the mean speeds and mean maximum speeds were also the same (Figure 8C and D). Thus, the rapid PC motions that begin when nuclei have unpaired chromosomes persist without change after the PC regions have successfully paired.

***X* Chromosome PCs remain mobile after synapsis of all chromosomes has been completed**

In *C. elegans,* when all chromosomes have completed synapsis with their homolog and entered the pachytene stage of meiotic prophase, chromosomes redistribute around the periphery of the nucleus making this stage cytologically distinct from the crescent-shaped chromosome conformation seen in the transition zone (examples in Figure 7). We took advantage of this distinction to examine the motion of *X* PCs specifically in pachytene nuclei. Again, we see that *X* PCs in pachytene nuclei

are much more dynamic than in premeiotic nuclei (Figure 7). The mean squared displacements for *X* PCs in pachytene nuclei are much higher than those in premeiotic nuclei (Figure 8A) and they have an mean speed of 0.055 ± 0.045 μm/s (n = 33 trajectories) compared to 0.039 ± 0.031 μm/s in premeiotic nuclei (Figure 8C). However, despite this increase in mobility compared to premeiotic nuclei, *X* PCs in pachytene nuclei do not show as dramatic an increase as those in transition zone nuclei, making them intermediate between these extremes. Both the mean squared displacements and the speed distributions plots for *X* PCs in pachytene nuclei roughly bisect the gaps between the plots for premeiotic nuclei and transition zone nuclei (Figure 8). The mean maximum speeds are 0.193 ± 0.049 μm/s for *X* PCs in pachytene nuclei which is well below the mean maximum speeds of roughly 0.3 μm/s measured in transition zone nuclei (Figure 8D). So, although it is clear that the increased mobility of *X* PCs that begins in the transition zone persists after synapsis is complete, the rapid motions show a significant decrease after nuclei have progressed into pachytene.

Meiotic Chromosome motion occurs primarily at the PC end

Having established that PCs are highly dynamic in meiotic nuclei I next wondered how much motion is present along the rest of the chromosome. To address this, I took advantage of a technique that can specifically label the X chromosome. Injection of fluorescently-labeled dUTP into the *C. elegans* gonad is specifically incorporated into *X* Chromosomes in a subset of nuclei (Jaramillo-Lambert et al., 2007), likely because the *X* chromosome is late replicating in these nuclei and injection follows replication of the autosomes. I injected worms expressing GFP::HIM-8 and mCherry::Histone with Cy5-dUTP and let worms recover 4-6 hours to allow nuclei with labeled *X* chromosomes to progress into the transition zone. In these nuclei the PC end of the chromosome is highly mobile while the remainder of the chromosome moves much less (Figure 9). The opposite end of the chromosome from the PC seemed to remain virtually immobile throughout data collection. To quantify this, I segmented *X* chromosomes using the signal from Cy5 incorporation and manually tracked the non-PC ends (Figure 9C). When compared to motion of the PCs, the distribution of speeds for non-PC ends was shifted down with a major peak around .03 μm/s and few motions greater than 0.1 μm/s, similar to that of X PCs in the premeiotic region (Figure 9C). The tracks for non-PC ends of *X* chromosomes consistently showed lower mean and mean maximum speeds when compared to the motion of the PC of that chromosome (Figure 9E). Interestingly, comparing PC motion to the motion of the non-PC end of the same chromosome showed a correlation: chromosomes that have faster PC motions also have faster non-PC chromosome-end motion, suggesting that force is being translated down the length of the chromosome.

X Chromosome imaging reveals that meiotic chromosomes are highly elastic

Surprisingly, when I visualized the *X* PCs along with the rest of the *X* Chromosome I noticed that the apparent chromosome length appears to be quite variable. In dramatic instances, it appears that the PC end can move far away from the mass of Cy5 signal and only later recover to a position at the end of the Cy5 signal (Figure 10). In Figure 9B, Cy5 signal can only faintly be seen between the site of the X PC and the bulk of the chromosome. The fact that the PC does return to the rest of the

Cy5 signal implies that there is force opposing the stretching of the chromosome and suggests that meiotic chromosomes may be quite elastic.

X PCs can fluctuate between being paired and unpaired

The observation that X PC motion is quite similar regardless of whether the PCs are paired or unpaired led me to question what types of transitions occur as chromosomes progress from being unpaired to being paired. Specifically, I wondered whether once pairing occurred between PCs if those PCs remained paired or, conversely, if PCs transition back and forth between being paired and unpaired. Looking through the live-imaging datasets I first noticed that in the majority of nuclei if X PCs were paired or unpaired in the first time point then they remained so throughout the 5 min. data collection (Figure 11A). This suggested either that pairing is indeed a one-way street, with PCs never coming unpaired once they pair, or that the periods between transitions, when nuclei are temporarily paired or unpaired, are normally much longer than our 5 min observations. I favor the former possibility both because of the number of 5 min datasets I have collected and because I have extended data collection for up to 30 min and have not seen these transitions.

Instead, I have observed a few nuclei in which the X PCs transition from being unpaired to paired and remain so (Figures 11B), or nuclei in which the X PCs become transiently unpaired and then pair (Figure 12A and B). In the first situation, it is exciting to think that I have captured the moment of pairing. However, I cannot rule out the possibility that these are temporary pairing events and that these PCs will not remain paired beyond data collection. In the second situation, what I saw most often was that the X PCs separate in only a single time point or two and appear to be stretching away from one another (Figure 12A). Less frequently, I caught a couple nuclei in which the X PCs separate for long enough to change direction and move separately from one another briefly before restoring their colocalization (Figure 12B). These data show that temporary colocalization of PCs is not sufficient for permanent pairing. Though that may occur in the majority of nuclei, these data present the possibility that there is a short intermediate stage in which PCs can transiently separate and have thus not yet achieved stable pairing.

Moreover, analysis of nuclei in which the X PCs are unpaired has provided no support for the idea that motion specifically promotes pairing. To test this, I calculated the change in distance between X PCs in successive time points, measuring whether they are getting closer of farther apart, and plotted those values against the speed at which each X PC moved in that span of time (Figure 12D). If fast motions tended to bring X PCs together, then there should be a negative correlation between these datasets, particularly for the fastest speeds. In contrast, the plot in Figure 12D shows that fast motions are just as likely to move X PCs away from one another as they are to bring them closer together.

Chapter III: Rapid Prophase Chromosome Motion in *C. elegans* is Driven by Dynein and the Microtubule Cytoskeleton

Summary

In this chapter I use the X Chromosome Pairing Center imaging established in Chapter II to investigate the role of cytoskeletal components in meiotic chromosome motion in *C. elegans*. I show that these infrequent, rapid motions occur in all nuclei with functional NE patches and that they are lost when dynein function is lost or MTs are disrupted with drugs. I also show that MTs surround meiotic nuclei in dense bundles that associate with some, but not all, meiotic NE patches. This work establishes that rapid prophase motions in *C. elegans* are specifically dependent on the MT cytoskeleton and suggests a model in which the intermittent rapid motions result from temporary association and dissociation between NE patches and MT filaments.

Introduction

In the two model organisms in which rapid prophase motions have been best characterized, *S. cerevisiae* and *S. pombe*, cytoskeletal components have been shown to provide the driving force for chromosome motion. However, in *S. cerevisiae*, motion is dependent on the actin cytoskeleton while motion in *S. pombe* relies on MTs (Ding et al., 1998; Trelles-Sticken et al., 2005). In addition, in maize rapid motion is sensitive to both actin and MT destabilizing drugs (Sheehan and Pawlowski, 2009). With the small number of model systems in which the cytoskeletal dependance of rapid motions has been addressed it is unclear which of these systems is the best conserved and which is more unusual. In *C. elegans*, the first clue that cytoskeletal components are involved in meiotic motion came from the observation that cytoplasmic dynein, a minus-end directed MT motor, could be seen by immunofluorescence to colocalize with meiotic NE patches (Sato et al., 2009). This fit well with earlier data showing that ZYG-12 can localize to the centrosome, the MT-organizing structure, and that the connection ZYG-12 mediates between the nucleus and the centrosome also depends on MTs (Malone et al., 2003). Further, Sato et al. showed that MT-depolymerizing drugs or loss of dynein function cause defects in pairing and synapsis, providing functional evidence for the role of the MT cytoskeleton in these processes.

In Chapter I, I presented quantitative analysis of motion showing that ZYG-12 motion is non-random, which suggests that it is not a result of simple diffusion but likely caused by active processes. Thus, the next major question was to directly address the extent to which these motions are driven by dynein and the MT cytoskeleton as suggested by the evidence from the analysis of fixed samples.

Results

Rapid *X* Chromosome PC movements are dependent on the presence of NE patches

Having shown that there is a class of rapid prophase motions specific to meiosis in *C. elegans*, the next major question is what causes these motions. As discussed above, it has been previously shown that NE proteins aggregate into patches in nuclei in the transition zone and that the formation of these NE components are required for normal pairing and synapsis. I predicted that the rapid *X* Chromosome PC motion I observed in the transition zone was dependent on the formation of these patches. To test this directly I first expressed GFP::HIM-8 and mCherry::Histone in animals mutant for the checkpoint kinase *chk-2,* which lack NE patches and the characteristic crescent-shaped nuclear morphology of the transition zone (MacQueen and Villeneuve, 2001). As predicted, *X* PCs throughout the gonad of *chk-2* mutants showed similar mobility as those in the premeiotic region of wild type animals both in terms of speed and displacement (Figure 13).

Similarly, I suspected that loss of SUN-1, the inner NE component of meiotic NE patches, would diminish rapid prophase motions. Expression of GFP::HIM-8 and mCherry::Histone in the *sun-1(jf18)* mutant confirmed that no rapid X PC motions are present. Interestingly, *sun-1(jf18)* mutants also exhibit precocious synapsis but there is no evidence that this limits the mobility of chromosomes as it does in wildtype animals.

In contrast to situations in which NE patches do not form, mutant situations exist in which the transition zone is extended and patch formation persists. Loss of the central element component SYP-1 causes this persistent NE patch phenotype so I expressed GFP::HIM-8 and mCherry::Histone in *syp-1(me16)* mutants to test whether rapid motions persist in an extended transition zone. As predicted, X PCs continue to show rapid motions throughout the extended transition zone in these mutants (Figure 13). Taken together, these mutant situations show a complete correlation between the presence of NE patches and rapid X PC motions, providing substantial validation for the model that the function of NE patches is to move chromosomes.

Dynein is required for rapid X PC motions

Because dynein localizes to meiotic NE patches and plays a necessary role in normal pairing and synapsis (Sato et al. 2009), I expected that the rapid prophase motions seen for the X PC would depend on dynein function. To test this, I assayed X PC mobility after knockdown of dynein motor function. To knockdown dynein function I used a combination of a temperature-sensitive point mutation in the dynein heavy chain gene, *dhc-1(or195)*, and RNAi targeting the dynein light chain gene *dlc-1* (O'Rourke et al., 2007). This treatment causes a strong defect in synapsis but only a delay in normal pairing with most X PCs able to pair by the end of the transition zone (88%, Sato et al., 2009). Because the effect on homologous pairing after dynein knockdown is mild, I expected a mild defect in motion following dynein knockdown. Interestingly, rapid X PC motions proved extremely sensitive to dynein knockdown (Figure 14). Quantification of the mean squared displacements and speed distributions verified this lack of motion after dynein knockdown (Figures 14C and D). The mean speed of X PCs following dynein knockdown was 0.034 ± 0.026 μm/s compared to control knockdowns that were

0.060 ± .034 μm/s and the maximum speeds mean 0.112 ± 0.013 μm/s for dynein knockdown and 0.212 ± 0.054 μm/s for controls (n = 45 trajectories for both dynein knockdown and control knockdown, Figures 14E and F). The lack of mobility after dynein knockdown is very similar to the amount of motion seen in premeiotic nuclei in wildtype animals, showing that all meiosis specific rapid motions depend on dynein.

Rapid prophase motions depend on microtubules but are unaffected by actin destabilizing drugs

Because dynein is a microtubule motor, the dependence of rapid X PC motions on dynein function suggested that these motions would depend on normal microtubule polymerization. To test this idea I first decided to examine the structure of microtubules around meiotic nuclei in *C. elegans*. To do so I combined a recently published MT fixation protocol *(Zhou et al., 2009)* with 3D structured illumination super-resolution florescence microscopy (Schermelleh *et al.* 2008, Gustafsson *et al.* 2008). Staining with anti-αTubulin antibodies showed a dense network of MTs surrounding meiotic nuclei (Figure 15). Co-staining of MTs and ZYG-12 protein showed that NE patches sometimes, but not always, associate with MTs. MTs do not appear to nucleate from NE patches but rather patches seem to form lateral associations with filaments that can extend beyond the end of the nucleus in both directions.

To directly address whether rapid X PC motions depend on MT I assayed X PC motion after depolymerization of MTs by microinjection of colchicine. Injection of 0.1M colchicine eliminated rapid X PC motions (Figures 16). Quantification validated that both displacement and speeds were greatly reduced after colchicine injection, to levels at or below that seen in premeiotic nuclei (n = 31 tracks for colchicine and 32 tracks for control injections, Figure 17). Mean and mean maximum speeds were likewise both reduced with maximum speeds reaching only 0.66 ± 0.018 μm/s compared to control, buffer-injected animals that had 0.194 ± 0.031 μm/s mean maximum speeds. Injection mixtures used in drug experiments also contained Cy5-dUTP which was used in this case as a control to allow us to select successfully injected animals.

Having seen a potent response in X PC motion to MT depolymerization I wondered if X PC motion was solely dependent on the MT cytoskeleton. To address whether the actin cytoskeleton is also required for normal X PC motion I injected animals with LatrunculinA. Following microinjection of 10 μM LatrunculinA, X PC motion was indistinguishable from motion in injected animals. The mean square displacement and speed distribution plots both overlapped remarkably well with that of control injections and both the mean speed (0.070 ± .054 μm/s) and mean maximum speed (0.221 ± .050 μm/s) was very close to that of controls (n = 24 trajectories, Figures 16 and 17). Thus, X PC motion appears to be much more sensitive to MT destabilizing drugs than to those that destabilize actin filaments.

Discussion

Rapid prophase motions are conserved in animals and display a combination of the features of meiotic motions seen in yeast

In this work I have shown that there is a class of rapid chromosome motions that are specific to meiotic prophase in *C. elegans*. This finding supports the notion that rapid chromosome motions are a well-conserved feature of meiotic prophase chromosome dynamics and that many of the observations of motion that have been made in yeast, where these motions have been most extensively studied, are conserved in animals. This work also helps to address which features of prophase chromosome motion, out of the variety of features that have been reported in different systems, are typically a part of the meiotic program. Interestingly, motion in *C. elegans* seems to be a combination of some features that have previously been seen specifically in *S. pombe* or *S. cerevisiae*. In all cases, chromosome motion has been end-directed, as I have found it is in *C. elegans,* but in *S. pombe* all telomeres remain clustered together and chromosomes are all moved in the same direction while in *S. cerevisiae* telomere clustering is transient and rapid motions move telomeres independently. Motion in *C. elegans*, in this regard, is much more similar to that of *S. cerevisiae*, because Pairing Centers are all moved independently and the interactions seen between PCs (as visualized by ZYG-12 patch localization) involve only a small number of NE patches at a time with no evidence of clustering. In contrast, although all motion is mediated through attachment to conserved NE complexes that connect chromosomes to cytoskeletal forces, the cytoskeletal components used in *C. elegans*, dynein and microtubules, are the same as those used in *S. pombe* rather than *S. cerevisiae.*

These observations suggest that the dependence of meiotic prophase motion on the MT cytoskeleton may be the ancestral state with the dependence on actin being derived in *S. cerevisiae*. However, the function of rapid prophase motions may be more typical in *S. cerevisiae* than in *S. pombe* because the nature of the movements is quite different between *S. pombe* and *C. elegans.* In *S. pombe* motion seems to specifically promote pairing by aligning homologous chromosomes and does not fit models in which motion serves to inhibit ectopic interactions, the stabilization of pairing, or to resolve interlocks. There is reason to believe these roles of meiotic motion could have been lost in the lineages like *S. pombe* where stabilization of pairing does not rely on the presence of a synaptonemal complex. Because *S. pombe* does not contain a central element that polymerizes between homologs and because it has only three chromosomes it also stands to reason that the formation of interlocks is not common. The motions that have been seen in *S. pombe* are most likely a unique elaboration of the chromosome bouquet conformation, which is quite distinct from the rapid motions characterized here and in *S. cerevisiae. S. pombe* seems to have lost this type of rapid motion.

Many major questions remain about the nature of rapid prophase motions. Future work is needed to address how force is generated and transduced to NE complexes to move chromosomes. Specifically, are MTs being polymerized at the sites of meiotic patches or do patches migrate along stable filaments? Similarly, does dynein remain attached to NE patches and walk along filaments and, if so, how processive are

these walks? To address these questions, more experiments must be done in which the interactions between patches and MTs can be visualized in live animals. Of particular interest would be to see if patch motion parallels an existing filament or moves at the end of a filament. A reporter for the localization of the *C. elegans* EB1 homolog *ebp-2*, a MT plus end binding protein, has been used to measure MT dynamics in *C. elegans* embryos and could be used similarly in meiosis *(Srayko et al., 2005)*. Interestingly, that study showed that MT filaments grow at speeds from 0.5 - 1.0 μm/s in embryos and they characterize a class of even faster, dynein-dependent motions that occur near the nuclear envelope during early prophase that they suggest are the result of free MT filaments being accelerated by NE-bound dynein. A combination of these two mechanisms could be responsible for rapid meiotic motion with the fastest motions being caused by growth of MTs that are themselves being moved. The fact that these MT dynamics are similar to the meiotic chromosome motions I characterized here means that further investigation of meiotic motions could help us understand not only closely related SUN/KASH complex functions but also may be applied to MT dynamics more generally.

Rapid motions in meiosis are likely to oppose non-homologous interactions and restrict synapsis to appropriately paired chromosomes

My observation of rapid prophase motions by visualizing both X Chromosome PCs and nuclear morphology allowed me to address how rapid motions correlate with pairing at the PC, and the completion of synapsis. It was clear using this approach that rapid motions are unaffected by paring. This shows that there is no specificity for unpaired chromosomes and suggests that rapid motion may play a role other than to pair chromosomes at the PCs. This observation is strengthened by the fact that rapid motions are as likely to move unpaired X PCs farther apart as they are to move them together. If the function of rapid motion is not to pair chromosomes then the major question remains, what is its function? One possibility, presented by Sato et al., is that rapid motions add stringency to the homology search. This model is based in large part on the observation that loss of dynein causes a loss of synapsis even in nuclei where the PCs has successfully paired. This result suggests that there is a barrier to synapsis that is overcome by dynein function. If only correctly paired PCs were able to resist the destabilizing force of rapid chromosome motions, this could prevent synapsis between inappropriately paired chromosomes. This model was favored over an alternate model in which rapid motions align chromosomes prior to synapsis and the alignment is required for synapsis even if pairing is achieved because there is no evidence of chromosome alignment before synapsis in *C. elegans.* Further, the barrier to synapsis in *C. elegans* appears to prevent all polymerization of central elements as no partial tracks are seen after dynein knockdown as might be expected if central element polymerization was being blocked by interlocks or regions where appropriate alignment has not been achieved. My observation that X PCs come apart briefly, often by stretching out over a very short time, provides support for the model in which rapid motions impose stringency because it suggests that even correctly paired chromosomes have to resist substantial destabilizing forces. However, future work is required to test this model more directly.

The most important test of this model will be to determine the kinetics of synapsis. This requires the development of an SC central element reporter which could then be used to visualize synapsis initiation in live animals. The prediction of the stringency model is that only a subset of paired PCs lead to synapsis initiation. Live imaging may reveal a correlation between rapid motion and synapsis initiation. Alternatively, another test that would discriminate between these models would be to mark both the PC and a locus farther down the chromosome. Perhaps no evidence has yet been found for presynaptic alignment in *C. elegans* because these events are transient. Live imaging would reveal the frequency with which non-PC loci pair and determine how this is affected by pairing at the PC. In both cases, the work presented here provides a launching point for future work and establishes *C. elegans* as a useful system for the live analysis of meiotic chromosome motion.

Methods

Generating Transgenic Reporters

The *phtp3:gfp::him-8* construct contains the *htp-3* promoter (488bp ending with the first 13 bases of the first exon of *htp-3*), the S65C GFP variant containing 3 synthetic introns (sequence taken from Fire lab vectors via the Seydoux lab vector kit) (Merritt and Seydoux), and the *him-8* genomic sequence including 1208bp downstream of the final exon. Fragments were combined into a single vector using the Multisite Gateway system, which left two *attB* recombination sequences at the junctions that were translated in the protein product. This construct was integrated into a site on chromosome *II* using the MosSCI transposon-mediated insertion system (Frokjaer-Jensen et al., 2008).

Strains

CA261 - *ojIs9*[*pie-1:GFP::zyg-12*] IV.
CA493 - *dhc-1(or195)* I ; *ojIs9*[*ppie-1*: *zyg-12::gfp*] *unc-24* IV.
CA756 - *ieSi1*[*cbunc119+ phtp-3:gfp::him-8*] II; *ltIs37*[*ppie-1:mCherry-TEV-Spep::his-58 unc119+*] IV.
CA777 - *ieSi1*[*phtp3:gfp::him-8 unc119+*] II; u*nc-119(ed3)*? III; *ltIs37*[*ppie-1:mCherry-TEV-Spep::his-58 unc119+*] *him-8(tm611)* IV.
CA778 - *ieSi1*[*phtp3:gfp::him8 unc-119+*] II; *unc119(ed3)*? III; *ltIs37*[*ppie-1:mCherry-TEV-Spep::his-58 unc-119+*] IV; *chk-2(me64) rol-9(sc148)*/*unc-51(e369) rol-9(sc148) V*.
CA786 - *ieSi1*[*phtp-3:gfp::him-8 unc-119+*] II; *ltIs37*[*ppie-1:mCherry-TEV-Spep::his-58 unc-119+*]/*nT1* IV; *syp-1(me17)*/*nT1*(*myo-2:gfp* and Unc) V.
CA805 - *dhc-1*(*or195ts*) I; *ieSi1*[*cbunc-119+ phtp-3:gfp::him-8*] II; *ltIs37*[*ppie-1:mCherry-TEV-Spep::his-58*, *unc-119+*] IV.
CA823 - *ieSi1*[*cbunc-119+ phtp-3:gfp::him-8*] II; *ltIs37*[*ppie-1:mCherry-TEV-Spep::his-58 unc119+*] IV; *sun-1(jf18)*/*nT1* (IV;V).

Time-lapse fluorescence microscopy

For live imaging of meiosis, young adult worms (16-20 hours post L4) were immobilized on freshly-made 3% agarose pads in a drop of M9 containing 0.4mM (0.05%) tetramisole and 3.8mM (0.5%) tricaine. A 1.5 coverslip was applied without sealing 2-5 min after immersion in anesthetic and data was collected 5-30 min after immersion. Wide-field fluorescence imaging was done using a DeltaVision RT microscope with either a 60x NA 1.2 UPlanApo or a 100x NA 1.4 UPlanSApo objective. On the OMX system excitation light was provided by a solid-state 488nm laser attenuated to 10% transmission with a neutral density filter. A piezoelectric stage provided rapid translation in Z, and an EMCCD camera (Andor Ixon) was used to record images at a frame rate of 30 Hz. Confocal microscopy was done using a Marianas digital microscopy workstation (Intelligent Imaging Innovations) equipped with a Yokogawa CSU-X1 spinning disk, Evolve EMCCD camera (Photometrics), 63x NA 1.4 PlanApo objective, and spherical aberration correction module.

Image Processing, Segmentation, and 4D tracking

OMX data was processed by constrained, iterative deconvolution using a measured point spread function (PSF) and time points were aligned using Priism software prior to segmentation. Confocal data was routinely segmented without deconvolution however constrained iterative deconvolution was done using Slidebook software (Intelligent Imaging Innovations) before generating projections for visualization.

Alignment of data from both confocal and DV imaging was done using Imaris software (Bitplane). For alignment, nuclei were segmented and tracked using the Spots function in Imaris with an expected diameter of 3.5 μm on the mCherry::Histone signal. Tracks from well-tracked nuclei were then used to align the data using the Correct Drift function. For all data, following alignment the ZYG-12:GFP or GFP::HIM-8 signal was segmented and tracked using the Spots function with an expected diameter of 0.4-0.5 μm. Automatically generated tracks were then corrected manually to eliminate inappropriate connections (including connections between foci in different nuclei or between foci of different size or intensity when more likely assignments were available) or multiple spots assigned to the same focus and to add spots when they were missed by the automatic segmentation. For the ZYG-12::GFP datasets, since the identity of a patch cannot be followed unambiguously beyond merging with another patch we generated trajectories according to the following three rules during the manual editing of tracks. First, multiple patches were only assigned to a single ZYG-12 focus if they merged into a single focus from multiple foci in an earlier time point or split into multiple foci in a subsequent time point. Second, patches were only tracked if they remained present as an individual for 10 time points (≥ 20 s). Third, when the connectivity between patches was ambiguous from time point to time point (typically because two patches were assigned to a single focus or two patches of similar size and brightness remained close together in successive time points) we favored connections that produced the least motion.

Curve fitting

Algorithms for calculating best fit normal distributions were written using MATLAB by generating datasets of 10,000 normally distributed random values with a given standard deviation and comparing these reference datasets to the experimental data. Cumulative distributions were calculated for the experimental and reference datasets and the dataset for which the sum of the absolute differences between these cumulative distributions was smallest was considered the bet fit. The same measure of fitness was used for comparison between experimental data and reference datasets representing two normal distributions.

Microinjections, drug treatments, and dynein knockdown

All microinjections were done into the distal gonad of young adult worms (16-20 hr post L4) with solutions containing 25nM Cy5-dUTP (GE Life Sciences) in injection buffer (20% PEG, mol. weight 6000-8000; 200mM potassium phosphate, pH 7.5; 30mM potassium citrate, pH 7.5). Colchicine was included at 100 mM and Latrunculin A was included at 10 μM with 2.5% DMSO. Dynein knockdown was achieved by a combination of RNAi against *dlc-1* and the temperature sensitive mutation *dhc-1(or195)* as described previously (O'Rourke et al., 2007; Sato et al., 2009).

Immunofluorescence and pairing analysis
Sample preparation and immunofluorescence were conducted as in (MacQueen et al., 2005). Quantification of pairing was done by dividing the transition zone region, as defined by ZIM-2 staining, into four segments of equal length. Foci were considered unpaired if they were over 0.5 μm apart.

Bibliography

Arya, G.H., Lodico, M.J., Ahmad, O.I., Amin, R., and Tomkiel, J.E. (2006). Molecular characterization of teflon, a gene required for meiotic autosome segregation in male Drosophila melanogaster. Genetics *174*, 125-134.

Bass, H.W., Riera-Lizarazu, O., Ananiev, E.V., Bordoli, S.J., Rines, H.W., Phillips, R.L., Sedat, J.W., Agard, D.A., and Cande, W.Z. (2000). Evidence for the coincident initiation of homolog pairing and synapsis during the telomere-clustering (bouquet) stage of meiotic prophase. J Cell Sci *113 (Pt 6)*, 1033-1042.

Berg, H.C. (1993). Random Walks in Biology (Princeton University Press).

Bhalla, N., Wynne, D.J., Jantsch, V., and Dernburg, A.F. (2008). ZHP-3 acts at crossovers to couple meiotic recombination with synaptonemal complex disassembly and bivalent formation in C. elegans. PLoS Genet *4*, e1000235.

Cheng, C.H., Lo, Y.H., Liang, S.S., Ti, S.C., Lin, F.M., Yeh, C.H., Huang, H.Y., and Wang, T.F. (2006). SUMO modifications control assembly of synaptonemal complex and polycomplex in meiosis of Saccharomyces cerevisiae. Genes Dev *20*, 2067-2081.

Chikashige, Y., Ding, D.Q., Funabiki, H., Haraguchi, T., Mashiko, S., Yanagida, M., and Hiraoka, Y. (1994). Telomere-led premeiotic chromosome movement in fission yeast. Science *264*, 270-273.

Chikashige, Y., Haraguchi, T., and Hiraoka, Y. (2007). Another way to move chromosomes. Chromosoma *116*, 497-505.

Chikashige, Y., Tsutsumi, C., Yamane, M., Okamasa, K., Haraguchi, T., and Hiraoka, Y. (2006). Meiotic proteins bqt1 and bqt2 tether telomeres to form the bouquet arrangement of chromosomes. Cell *125*, 59-69.

Chikashige, Y., Yamane, M., Okamasa, K., Tsutsumi, C., Kojidani, T., Sato, M., Haraguchi, T., and Hiraoka, Y. (2009). Membrane proteins Bqt3 and -4 anchor telomeres to the nuclear envelope to ensure chromosomal bouquet formation. J Cell Biol *187*, 413-427.

Chua, P.R., and Roeder, G.S. (1997). Tam1, a telomere-associated meiotic protein, functions in chromosome synapsis and crossover interference. Genes Dev *11*, 1786-1800.

Conrad, M.N., Dominguez, A.M., and Dresser, M.E. (1997). Ndj1p, a meiotic telomere protein required for normal chromosome synapsis and segregation in yeast. Science *276*, 1252-1255.

Conrad, M.N., Lee, C.Y., Chao, G., Shinohara, M., Kosaka, H., Shinohara, A., Conchello, J.A., and Dresser, M.E. (2008). Rapid telomere movement in meiotic prophase is promoted by NDJ1, MPS3, and CSM4 and is modulated by recombination. Cell *133*, 1175-1187.

Conrad, M.N., Lee, C.Y., Wilkerson, J.L., and Dresser, M.E. (2007). MPS3 mediates meiotic bouquet formation in Saccharomyces cerevisiae. Proc Natl Acad Sci U S A *104*, 8863-8868.

Cooper, J.P., Watanabe, Y., and Nurse, P. (1998). Fission yeast Taz1 protein is required for meiotic telomere clustering and recombination. Nature *392*, 828-831.

Corredor, E., Lukaszewski, A.J., Pachon, P., Allen, D.C., and Naranjo, T. (2007). Terminal regions of wheat chromosomes select their pairing partners in meiosis. Genetics *177*, 699-706.

Dernburg, A.F., McDonald, K., Moulder, G., Barstead, R., Dresser, M., and Villeneuve, A.M. (1998). Meiotic recombination in C. elegans initiates by a conserved mechanism and is dispensable for homologous chromosome synapsis. Cell *94*, 387-398.

Dernburg, A.F., Sedat, J.W., and Hawley, R.S. (1996). Direct evidence of a role for heterochromatin in meiotic chromosome segregation. Cell *86*, 135-146.

Ding, D.Q., Chikashige, Y., Haraguchi, T., and Hiraoka, Y. (1998). Oscillatory nuclear movement in fission yeast meiotic prophase is driven by astral microtubules, as revealed by continuous observation of chromosomes and microtubules in living cells. J Cell Sci *111 (Pt 6)*, 701-712.

Ding, D.Q., Yamamoto, A., Haraguchi, T., and Hiraoka, Y. (2004). Dynamics of homologous chromosome pairing during meiotic prophase in fission yeast. Dev Cell *6*, 329-341.

Ding, X., Xu, R., Yu, J., Xu, T., Zhuang, Y., and Han, M. (2007). SUN1 is required for telomere attachment to nuclear envelope and gametogenesis in mice. Dev Cell *12*, 863-872.

Fransz, P., De Jong, J.H., Lysak, M., Castiglione, M.R., and Schubert, I. (2002). Interphase chromosomes in Arabidopsis are organized as well defined chromocenters from which euchromatin loops emanate. Proc Natl Acad Sci U S A *99*, 14584-14589.

Frokjaer-Jensen, C., Davis, M.W., Hopkins, C.E., Newman, B.J., Thummel, J.M., Olesen, S.P., Grunnet, M., and Jorgensen, E.M. (2008). Single-copy insertion of transgenes in Caenorhabditis elegans. Nat Genet *40*, 1375-1383.

Fung, J.C., Rockmill, B., Odell, M., and Roeder, G.S. (2004). Imposition of crossover interference through the nonrandom distribution of synapsis initiation complexes. Cell *116*, 795-802.

Giroux, C.N., Dresser, M.E., and Tiano, H.F. (1989). Genetic control of chromosome synapsis in yeast meiosis. Genome *31*, 88-94.

Goldstein, P., and Slaton, D.E. (1982). The synaptonemal complexes of caenorhabditis elegans: comparison of wild-type and mutant strains and pachytene karyotype analysis of wild-type. Chromosoma *84*, 585-597.

Golubovskaya, I.N., Harper, L.C., Pawlowski, W.P., Schichnes, D., and Cande, W.Z. (2002). The pam1 gene is required for meiotic bouquet formation and efficient homologous synapsis in maize (Zea mays L.). Genetics *162*, 1979-1993.

Hawley, R.S. (1980). Chromosomal sites necessary for normal levels of meiotic recombination in Drosophila melanogaster. I. Evidence for and mapping of the sites. Genetics *94*, 625-646.

Hiraoka, Y., and Dernburg, A.F. (2009). The SUN rises on meiotic chromosome dynamics. Dev Cell *17*, 598-605.

Hodgkin, J., Horvitz, H.R., and Brenner, S. (1979). Nondisjunction Mutants of the Nematode CAENORHABDITIS ELEGANS. Genetics *91*, 67-94.

Hooker, G.W., and Roeder, G.S. (2006). A Role for SUMO in meiotic chromosome synapsis. Curr Biol *16*, 1238-1243.

Jaramillo-Lambert, A., Ellefson, M., Villeneuve, A.M., and Engebrecht, J. (2007). Differential timing of S phases, X chromosome replication, and meiotic prophase in the C. elegans germ line. Dev Biol *308*, 206-221.
Jin, Q., Trelles-Sticken, E., Scherthan, H., and Loidl, J. (1998). Yeast nuclei display prominent centromere clustering that is reduced in nondividing cells and in meiotic prophase. J Cell Biol *141*, 21-29.
Karpen, G.H., Le, M.H., and Le, H. (1996). Centric heterochromatin and the efficiency of achiasmate disjunction in Drosophila female meiosis. Science *273*, 118-122.
Koszul, R., Kim, K.P., Prentiss, M., Kleckner, N., and Kameoka, S. (2008). Meiotic chromosomes move by linkage to dynamic actin cables with transduction of force through the nuclear envelope. Cell *133*, 1188-1201.
Koszul, R., and Kleckner, N. (2009). Dynamic chromosome movements during meiosis: a way to eliminate unwanted connections? Trends Cell Biol *19*, 716-724.
Lei, K., Zhang, X., Ding, X., Guo, X., Chen, M., Zhu, B., Xu, T., Zhuang, Y., Xu, R., and Han, M. (2009). SUN1 and SUN2 play critical but partially redundant roles in anchoring nuclei in skeletal muscle cells in mice. Proc Natl Acad Sci U S A *106*, 10207-10212.
Leu, J.Y., Chua, P.R., and Roeder, G.S. (1998). The meiosis-specific Hop2 protein of S. cerevisiae ensures synapsis between homologous chromosomes. Cell *94*, 375-386.
MacQueen, A.J., Phillips, C.M., Bhalla, N., Weiser, P., Villeneuve, A.M., and Dernburg, A.F. (2005). Chromosome sites play dual roles to establish homologous synapsis during meiosis in C. elegans. Cell *123*, 1037-1050.
Macqueen, A.J., and Roeder, G.S. (2009). Fpr3 and Zip3 ensure that initiation of meiotic recombination precedes chromosome synapsis in budding yeast. Curr Biol *19*, 1519-1526.
MacQueen, A.J., and Villeneuve, A.M. (2001). Nuclear reorganization and homologous chromosome pairing during meiotic prophase require C. elegans chk-2. Genes Dev *15*, 1674-1687.
Maguire, M.P. (1986). The pattern of pairing that is effective for crossing over in complex B-A chromosome rearrangements in maize. III. Possible evidence for pairing centers. Chromosoma *94*, 71-85.
Malone, C.J., Fixsen, W.D., Horvitz, H.R., and Han, M. (1999). UNC-84 localizes to the nuclear envelope and is required for nuclear migration and anchoring during C. elegans development. Development *126*, 3171-3181.
Malone, C.J., Misner, L., Le Bot, N., Tsai, M.C., Campbell, J.M., Ahringer, J., and White, J.G. (2003). The C. elegans hook protein, ZYG-12, mediates the essential attachment between the centrosome and nucleus. Cell *115*, 825-836.
Martinez-Perez, E., Shaw, P., and Moore, G. (2001). The Ph1 locus is needed to ensure specific somatic and meiotic centromere association. Nature *411*, 204-207.
Martinez-Perez, E., and Villeneuve, A.M. (2005). HTP-1-dependent constraints coordinate homolog pairing and synapsis and promote chiasma formation during C. elegans meiosis. Genes Dev *19*, 2727-2743.
McKee, B.D., Habera, L., and Vrana, J.A. (1992). Evidence that intergenic spacer repeats of Drosophila melanogaster rRNA genes function as X-Y pairing sites in

male meiosis, and a general model for achiasmatic pairing. Genetics *132*, 529-544.
McKee, B.D., and Karpen, G.H. (1990). Drosophila ribosomal RNA genes function as an X-Y pairing site during male meiosis. Cell *61*, 61-72.
McKim, K.S., Howell, A.M., and Rose, A.M. (1988). The effects of translocations on recombination frequency in Caenorhabditis elegans. Genetics *120*, 987-1001.
Merritt, C., and Seydoux, G. Transgenic solutions for the germline. In WormBook, T.C.e.R. Community, ed. (WormBook).
Miki, F., Okazaki, K., Shimanuki, M., Yamamoto, A., Hiraoka, Y., and Niwa, O. (2002). The 14-kDa dynein light chain-family protein Dlc1 is required for regular oscillatory nuclear movement and efficient recombination during meiotic prophase in fission yeast. Mol Biol Cell *13*, 930-946.
Minn, I.L., Rolls, M.M., Hanna-Rose, W., and Malone, C.J. (2009). SUN-1 and ZYG-12, mediators of centrosome-nucleus attachment, are a functional SUN/KASH pair in Caenorhabditis elegans. Mol Biol Cell *20*, 4586-4595.
Morelli, M.A., Werling, U., Edelmann, W., Roberson, M.S., and Cohen, P.E. (2008). Analysis of meiotic prophase I in live mouse spermatocytes. Chromosome Res *16*, 743-760.
Nimmo, E.R., Pidoux, A.L., Perry, P.E., and Allshire, R.C. (1998). Defective meiosis in telomere-silencing mutants of Schizosaccharomyces pombe. Nature *392*, 825-828.
O'Rourke, S.M., Dorfman, M.D., Carter, J.C., and Bowerman, B. (2007). Dynein modifiers in C. elegans: light chains suppress conditional heavy chain mutants. PLoS Genet *3*, e128.
Parvinen, M., and Soderstrom, K.O. (1976). Chromosome rotation and formation of synapsis. Nature *260*, 534-535.
Penkner, A., Tang, L., Novatchkova, M., Ladurner, M., Fridkin, A., Gruenbaum, Y., Schweizer, D., Loidl, J., and Jantsch, V. (2007). The nuclear envelope protein Matefin/SUN-1 is required for homologous pairing in C. elegans meiosis. Dev Cell *12*, 873-885.
Pfeifer, C., Scherthan, H., and Thomsen, P.D. (2003). Sex-specific telomere redistribution and synapsis initiation in cattle oogenesis. Dev Biol *255*, 206-215.
Phillips, C.M., and Dernburg, A.F. (2006). A family of zinc-finger proteins is required for chromosome-specific pairing and synapsis during meiosis in C. elegans. Dev Cell *11*, 817-829.
Phillips, C.M., Wong, C., Bhalla, N., Carlton, P.M., Weiser, P., Meneely, P.M., and Dernburg, A.F. (2005). HIM-8 binds to the X chromosome pairing center and mediates chromosome-specific meiotic synapsis. Cell *123*, 1051-1063.
Praitis, V., Casey, E., Collar, D., and Austin, J. (2001). Creation of low-copy integrated transgenic lines in Caenorhabditis elegans. Genetics *157*, 1217-1226.
Romanienko, P.J., and Camerini-Otero, R.D. (2000). The mouse Spo11 gene is required for meiotic chromosome synapsis. Mol Cell *6*, 975-987.
Sato, A., Isaac, B., Phillips, C.M., Rillo, R., Carlton, P.M., Wynne, D.J., Kasad, R.A., and Dernburg, A.F. (2009). Cytoskeletal forces span the nuclear envelope to coordinate meiotic chromosome pairing and synapsis. Cell *139*, 907-919.

Schaner, C., and Kelly, W.G. Germline chromatin. In WormBook, T.C.e.R. Community, ed. (Worm'ook).
Scherthan, H. (2001). A bouquet makes ends meet. Nat Rev Mol Cell Biol *2*, 621-627.
Scherthan, H., Bahler, J., and Kohli, J. (1994). Dynamics of chromosome organization and pairing during meiotic prophase in fission yeast. J Cell Biol *127*, 273-285.
Scherthan, H., Wang, H., Adelfalk, C., White, E.J., Cowan, C., Cande, W.Z., and Kaback, D.B. (2007). Chromosome mobility during meiotic prophase in Saccharomyces cerevisiae. Proc Natl Acad Sci U S A *104*, 16934-16939.
Scherthan, H., Weich, S., Schwegler, H., Heyting, C., Harle, M., and Cremer, T. (1996). Centromere and telomere movements during early meiotic prophase of mouse and man are associated with the onset of chromosome pairing. J Cell Biol *134*, 1109-1125.
Sheehan, M.J., and Pawlowski, W.P. (2009). Live imaging of rapid chromosome movements in meiotic prophase I in maize. Proc Natl Acad Sci U S A *106*, 20989-20994.
Smolikov, S., Schild-Prufert, K., and Colaiacovo, M.P. (2008). CRA-1 uncovers a double-strand break-dependent pathway promoting the assembly of central region proteins on chromosome axes during C. elegans meiosis. PLoS Genet *4*, e1000088.
Soltani-Bejnood, M., Thomas, S.E., Villeneuve, L., Schwartz, K., Hong, C.S., and McKee, B.D. (2007). Role of the mod(mdg4) common region in homolog segregation in Drosophila male meiosis. Genetics *176*, 161-180.
Srayko, M., Kaya, A., Stamford, J., and Hyman, A.A. (2005). Identification and characterization of factors required for microtubule growth and nucleation in the early C. elegans embryo. Dev Cell *9*, 223-236.
Starr, D.A., and Fischer, J.A. (2005). KASH 'n Karry: the KASH domain family of cargo-specific cytoskeletal adaptor proteins. Bioessays *27*, 1136-1146.
Storlazzi, A., Gargano, S., Ruprich-Robert, G., Falque, M., David, M., Kleckner, N., and Zickler, D. (2010). Recombination proteins mediate meiotic spatial chromosome organization and pairing. Cell *141*, 94-106.
Tang, X., Jin, Y., and Cande, W.Z. (2006). Bqt2p is essential for initiating telomere clustering upon pheromone sensing in fission yeast. J Cell Biol *173*, 845-851.
Thomas, S.E., Soltani-Bejnood, M., Roth, P., Dorn, R., Logsdon, J.M., Jr., and McKee, B.D. (2005). Identification of two proteins required for conjunction and regular segregation of achiasmate homologs in Drosophila male meiosis. Cell *123*, 555-568.
Tomkiel, J.E., Wakimoto, B.T., and Briscoe, A., Jr. (2001). The teflon gene is required for maintenance of autosomal homolog pairing at meiosis I in male Drosophila melanogaster. Genetics *157*, 273-281.
Trelles-Sticken, E., Adelfalk, C., Loidl, J., and Scherthan, H. (2005). Meiotic telomere clustering requires actin for its formation and cohesin for its resolution. J Cell Biol *170*, 213-223.
Tsubouchi, T., and Roeder, G.S. (2005). A synaptonemal complex protein promotes homology-independent centromere coupling. Science *308*, 870-873.
Vazquez, J., Belmont, A.S., and Sedat, J.W. (2002). The dynamics of homologous chromosome pairing during male Drosophila meiosis. Curr Biol *12*, 1473-1483.

Villeneuve, A.M. (1994). A cis-acting locus that promotes crossing over between X chromosomes in Caenorhabditis elegans. Genetics *136*, 887-902.
Vogel, S.K., Pavin, N., Maghelli, N., Julicher, F., and Tolic-Norrelykke, I.M. (2009). Self-organization of dynein motors generates meiotic nuclear oscillations. PLoS Biol *7*, e1000087.
Walenta, J.H., Didier, A.J., Liu, X., and Kramer, H. (2001). The Golgi-associated hook3 protein is a member of a novel family of microtubule-binding proteins. J Cell Biol *152*, 923-934.
Wang, C.J., Carlton, P.M., Golubovskaya, I.N., and Cande, W.Z. (2009). Interlock formation and coiling of meiotic chromosome axes during synapsis. Genetics *183*, 905-915.
Zhou, K., Rolls, M.M., Hall, D.H., Malone, C.J., and Hanna-Rose, W. (2009). A ZYG-12-dynein interaction at the nuclear envelope defines cytoskeletal architecture in the C. elegans gonad. J Cell Biol *186*, 229-241.
Zickler, D., and Kleckner, N. (1998). The leptotene-zygotene transition of meiosis. Annu Rev Genet *32*, 619-697.

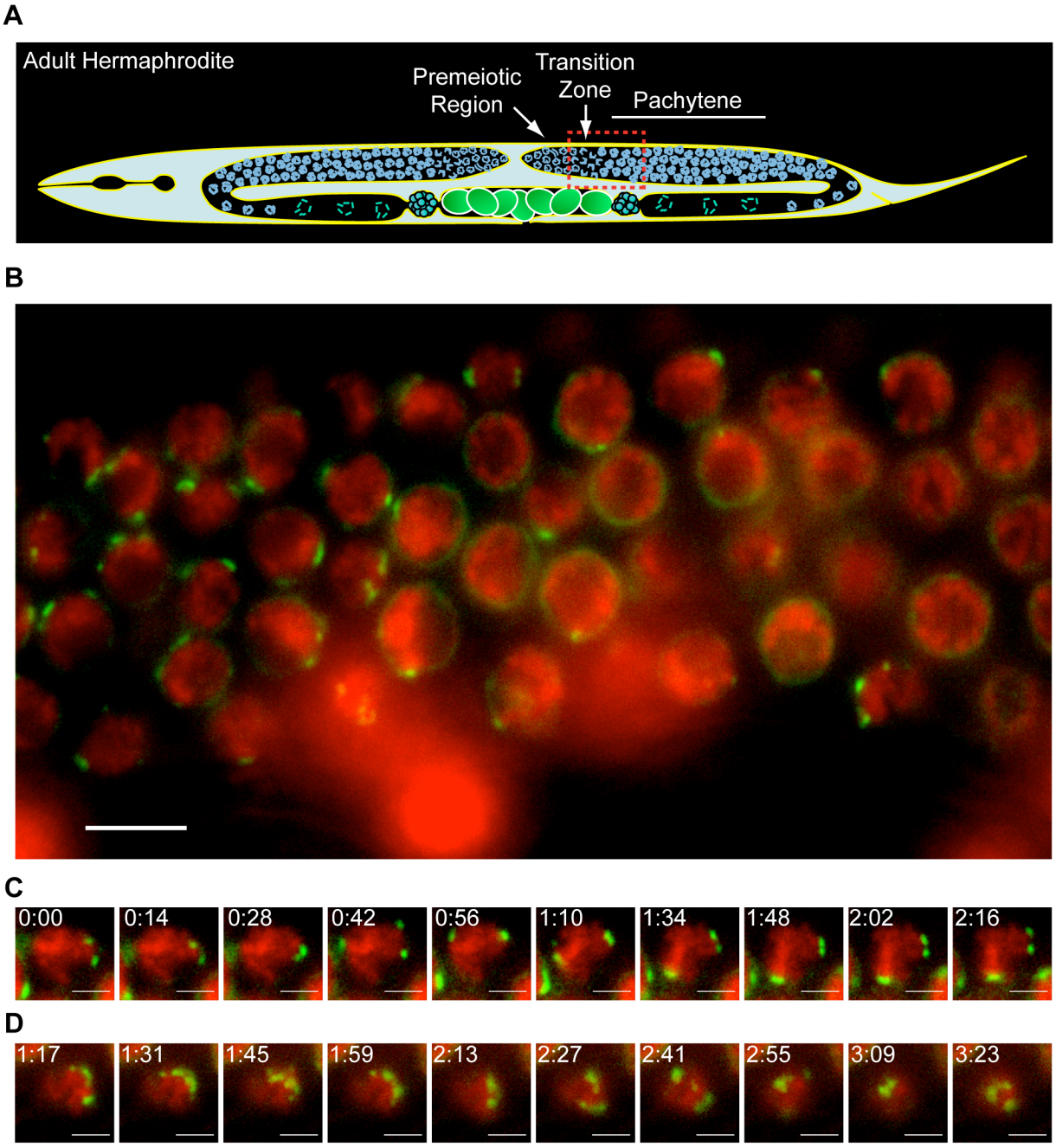

Figure 1. Meiotic nuclear envelope patches are highly dynamic in the transition zone.
(A) Schematic of the anatomy of the adult Hermaphrodite gonad emphasizing the chromosome morphology of meiotic nuclei. Stages relevant to the data presented are labeled. Outlined in the red box is the approximate field of view of the data shown in (B).
(B) Single optical section showing ZYG-12::GFP (green) and mCherry::Histone (red) in a section of the gonad in which nuclei in the transition zone can be seen on the left with early pachytene nuclei on the right.
(C and D) Time lapse series of single optical sections showing individual nuclei from the field shown in (B). In (C) the focal plane is in the middle of a transition zone nucleus while in (D) the focal plane is closer to top of the nucleus.

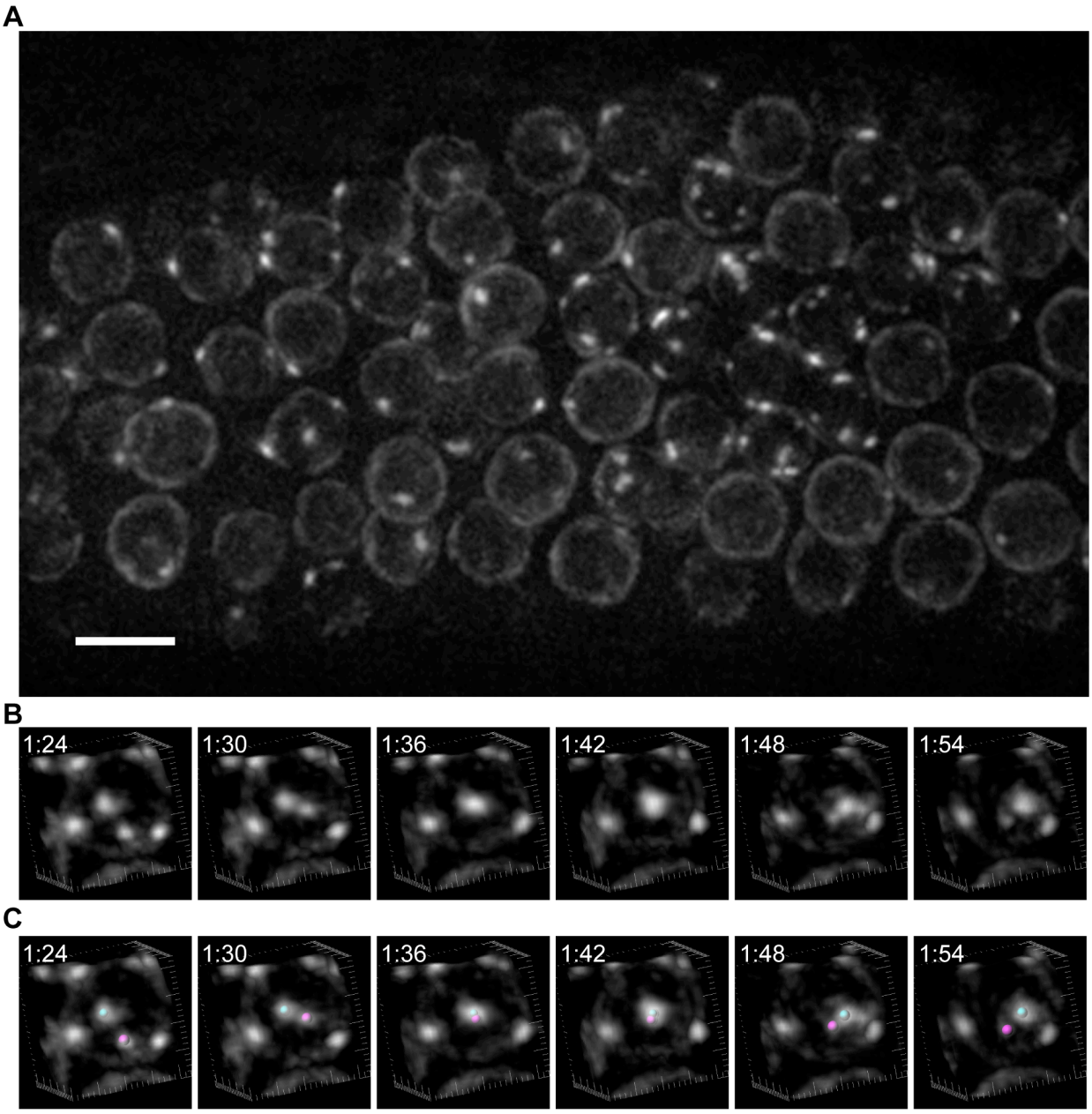

Figure 2. High resolution 4D imaging reveals that nuclear envelope patches merge and split.
(A) Projection of 25 optical sections (6 μm Z distance) showing ZYG-12::GFP signal in Transition Zone nuclei. Meiotic progression is towards the right, with nuclei earlier in meiosis on the left. (Scale bar = 5 μm)
(B-C) Time lapse series of projection images of a single nucleus from the field shown in (A). Colored spheres in (C) show the segmentation of patches that was used for tracking.
(D) Tracks representing the motion of the two patches segmented in (C) during the 2 min time course are shown superimposed on a single timepoint projection of the nucleus. (Large tick marks in (B)-(D) are 1 μm apart)

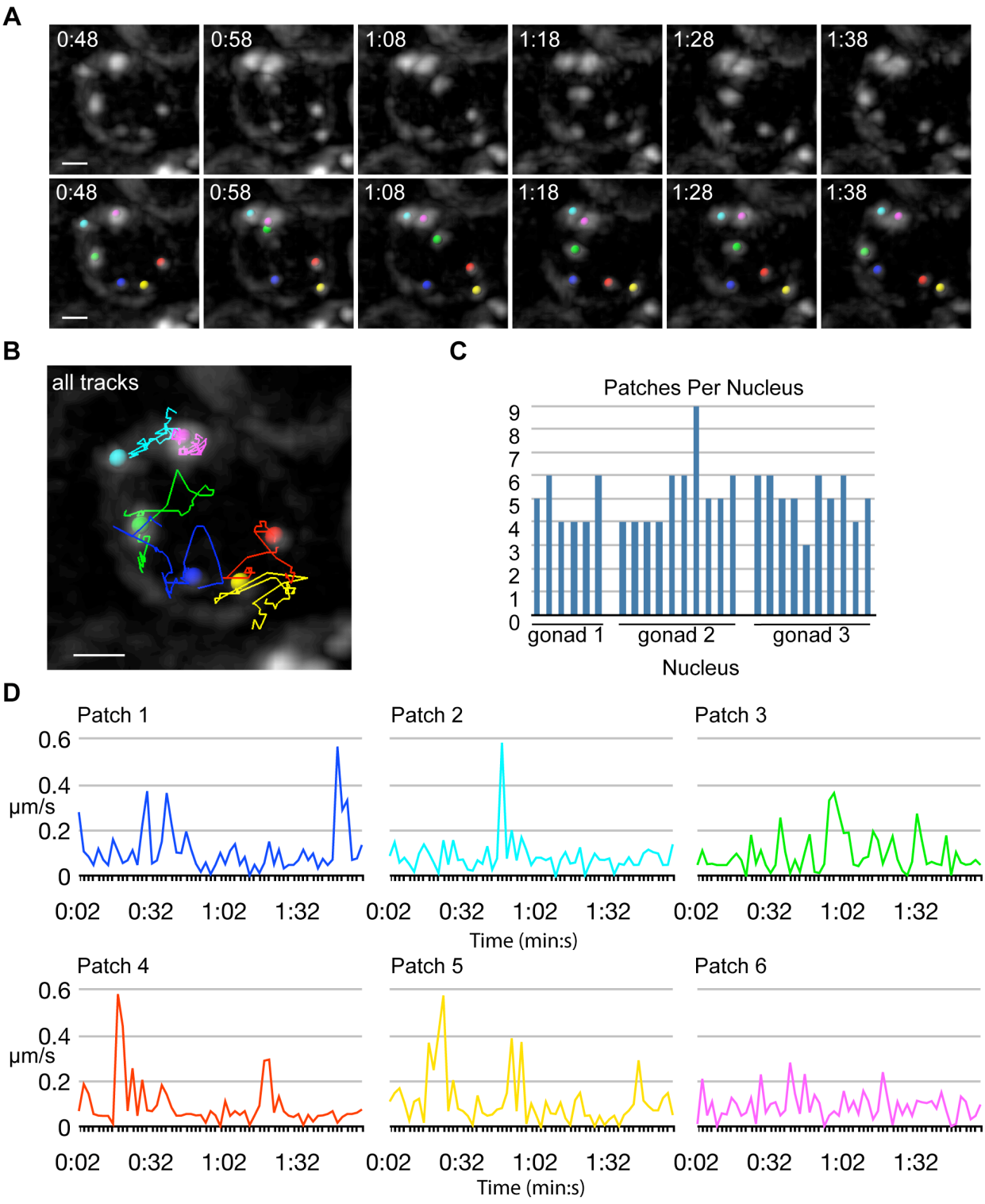

Figure 3. Quantification of the number and speed of meiotic nuclear envelope patches. (A) Timelapse series showing a nucleus with 6 ZYG-12 patches (above) and overlays of the segmentation used for tracking (below). (B) Colored tracks indicate all motion for patches shown in (A) over a 2min timecourse. (C) The nulber of ZYG-12 patches tracked per nucleus in the complete ZYG-12 dataset. (D) Plots depicting speed between each image collection for patches shown in (A) and (B). Scale bars = 1 µm

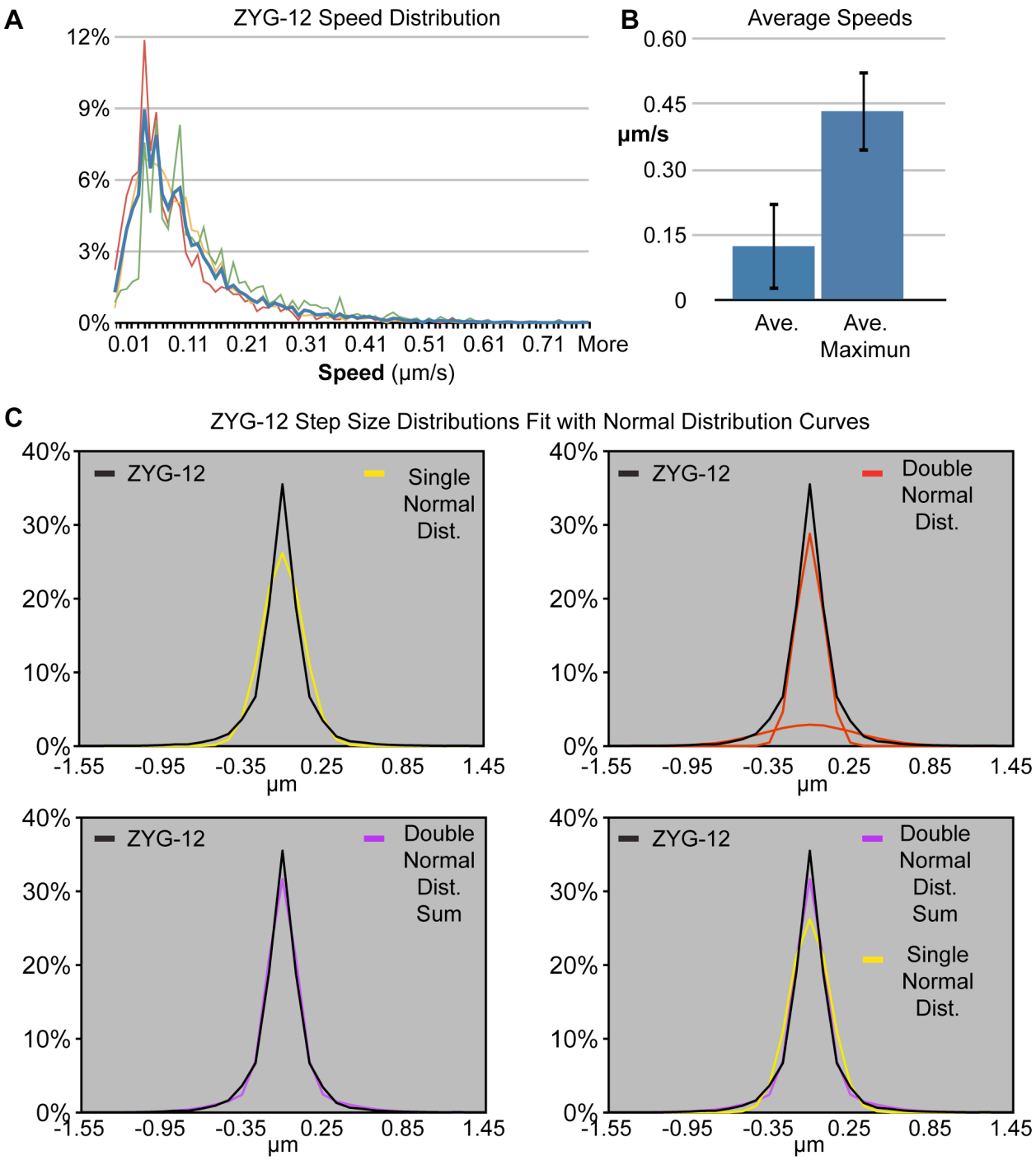

Figure 4. Nuclear envelope patch motion is unlikely to be a result of diffusion.
(A) Histogram of all speeds of ZYG-12 patches (blue) and for the patches from each gonad individually (red, yellow, green).
(B) Average and Average top 5% of speeds for all ZYG-12 patches. Error bars indicate standard deviation.
(C) Histogram of all ZYG-12 stepsizes (individual displacements in X, Y, and Z between all timepoints) fit with a single normal distribution (yellow) or a combination of two normal distributions (red) illustrating that the sum of two normal distributions (purple) provides a better fit for the data than a single normal distribution.

construct	# of integrants	expressed by IF	visible fluor.	strain names
pDJW1 - *ppie-1:mCherry-TEV-Spep::him-8* (pAA65 vector)	10	3	0	*ieIs16, 17,18*
pDJW2 - *ppie-1:mCherry-TEV-Spep::zim-2* (pAA65 vector)	2	0	0	*ieIs19, 20*
pDJW3 - *ppie-1:mCherry-TEV-Spep::zim-3* (pAA65 vector)	6	2	0	*ieIs21, 22*
pDJW4 - *ppie-1:gfp::him-8* (pCG150 vector)	7	ND	7	*ieIs24*
pDJW28 - *pzim-1:gfp::zim-2* (pCFJ150 vector)	5	ND	0	none
pDJW30 - *phtp-3:gfp::htp-1* (pCFJ150 vector)	ND	ND	1	*ieIs25*
pDJW31 - *phtp-3:gfp::syp-1* (pCFJ150 vector)	ND	ND	4	none
pDJW37 - *phtp-3:tdTomato::him-8* (pCFJ150 vector)	2	ND	0	none
pDJW38 - *phtp-3:tdTomato::zim-2* (pCFJ150 vector)	3	ND	0	none
pDJW43 - *ppie-1:tdTomato::him-8* (pCFJ150 vector)	2	ND	2	*ieIs26*
pDJW44 - *ppie-1:tagRFP-T::him-8* (pCFJ150 vector)	5	ND	1	none
pDJW47 - *ppie-1:gfp::zim-2* (pCG150 vector)	2	ND	0	none
pDJW48 - *ppie-1:emerald::zim-2* (pCG150 vector)	11	ND	0	none
pDJW50 - *ppie-1:tagRFP-T::zim-2* (pCG150 vector)	4	ND	0	none
pDJW51 - *ppie-1:tdTomato::syp-1* (pCG150 vector)	6	ND	0	none
pDJW52 - *ppie-1:tagRFP-T::syp-1* (pCG150 vector)	3	ND	0	none
pDJW63 - *phtp-3:emerald::htp-3* (pCG150 vector)	4	ND	2	none

Table 1. Results of transgene expression using biolistic transformation.
Expression of transgene constructs was judged by the production lines in which 100% of animals express the visible transgene marker *unc-119+* (“# of integrants”). These lines were then scored for germline expression of the fluorophore-tagged protein using either immunofluorescence with antibodies recognizing the fluorophore (“expressed by IF”) or fluorescent imaging of live animals (“visible fluorescence”).

A

construct	# injected animals with F2 transformants	Integrations by PCR	visible GFP
pDJW26 - *phtp-3:gfp::him-8* (pCFJ150 vector)	29	2	1
pDJW27 - *prad-51:gfp::him-8* (pCFJ150 vector)	78	13	1
pDJW28 - *pzim-1:gfp::zim-2* (pCFJ150 vector)	64	5	0
pDJW29 - *pzim-1:gfp::zim-3* (pCFJ150 vector)	45	1	0

B

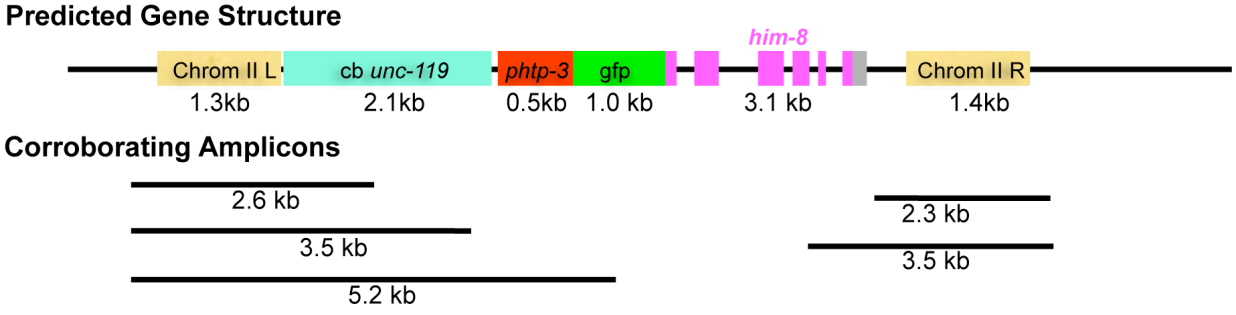

Figure 5. Transposon mediated homologous recombination was used to generate a low copy insertion into a specific locus.
(A) Table showing the success of integration using the MosSCI system (Frokjaer-Jensen et al. 2008).
(B) Illustration of the GFP-HIM-8 transgene used in this study (above) with the locations of PCR products used to validate the majority of the gene structure (below).

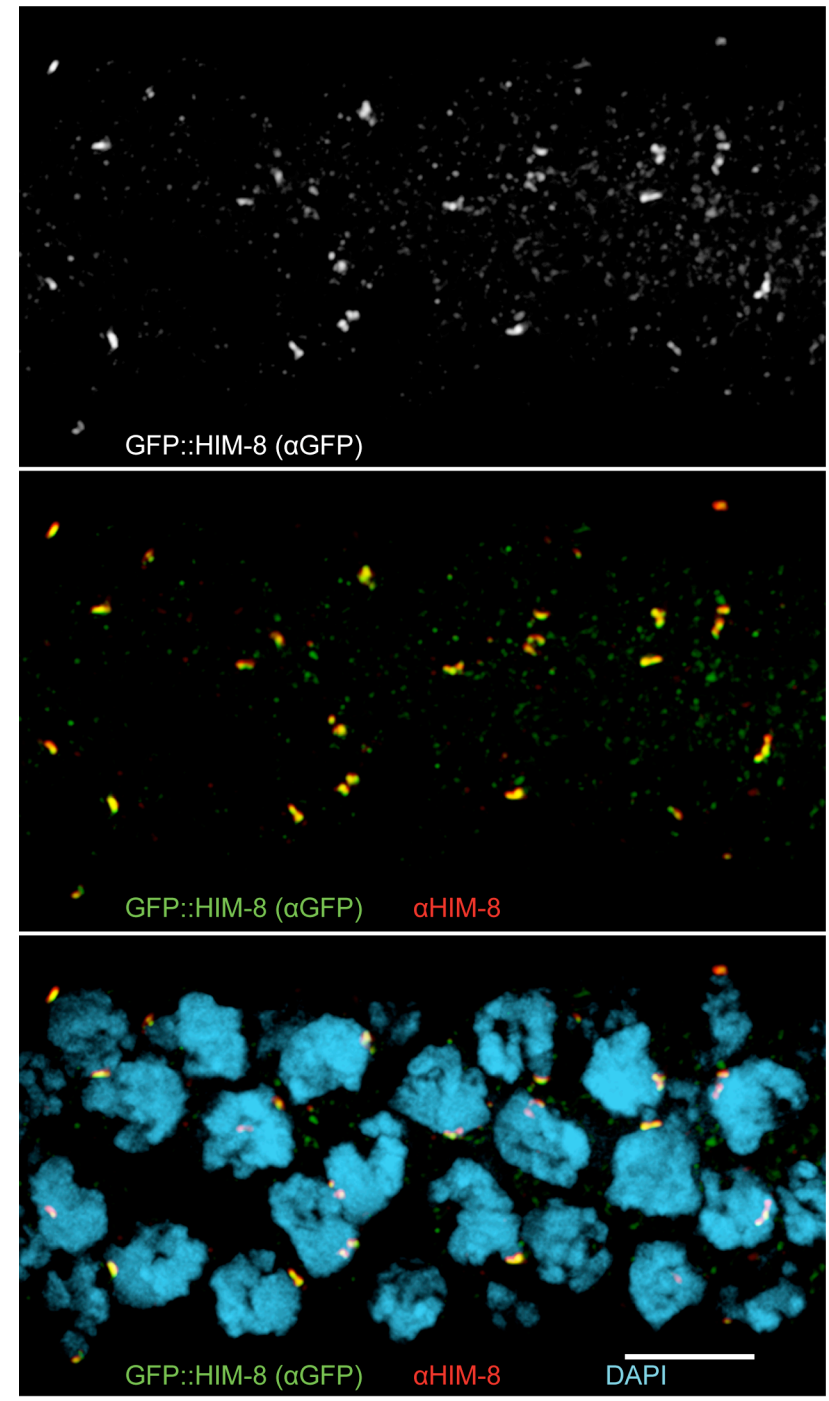

B

	% males
wild type (N2)	0.1 (2/1954)*
phtp-3:gfp::him-8	0.2 (3/1849)
him-8(tm611)	38.5 (422/1096)
phtp-3:gfp::him-8; *him-8(tm611)*	32.2 (845/2628)
phtp-3:gfp::him-8; *him-8(tm611)* @25°	29.9 (203/679)

*Phillips et al. 2005

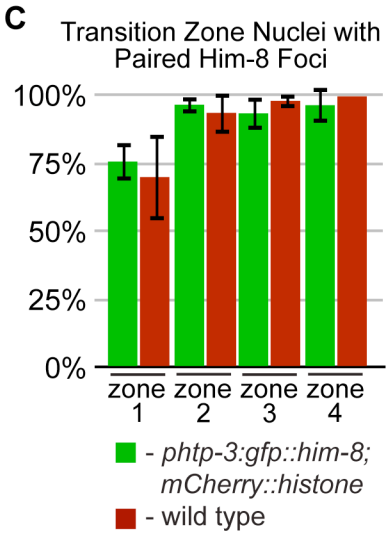

Figure 6. GFP::HIM-8 localizes to the X chromosome Pairing Center and does not interfere with X chromosome pairing or segregation.

(A) Projection image of transition zone nuclei stained with antibodies against GFP (top panel white, middle and bottom panels green) and HIM-8 (red) and with DAPI (blue). Scale bar = 5 μm.

(B) Frequency of male progeny in strains expressing GFP::HIM-8 (*phtp-3:gfp::him-8*) as an indicator of X chromosome nondisjunction.

(C) Quantification of X Chromosome pairing at the PC in animals expressing GFP::HIM-8 and mCherry::Histone. The transition zone regions of three gonads were divded into four equal-length sections. Error bars indicate standard deviation.

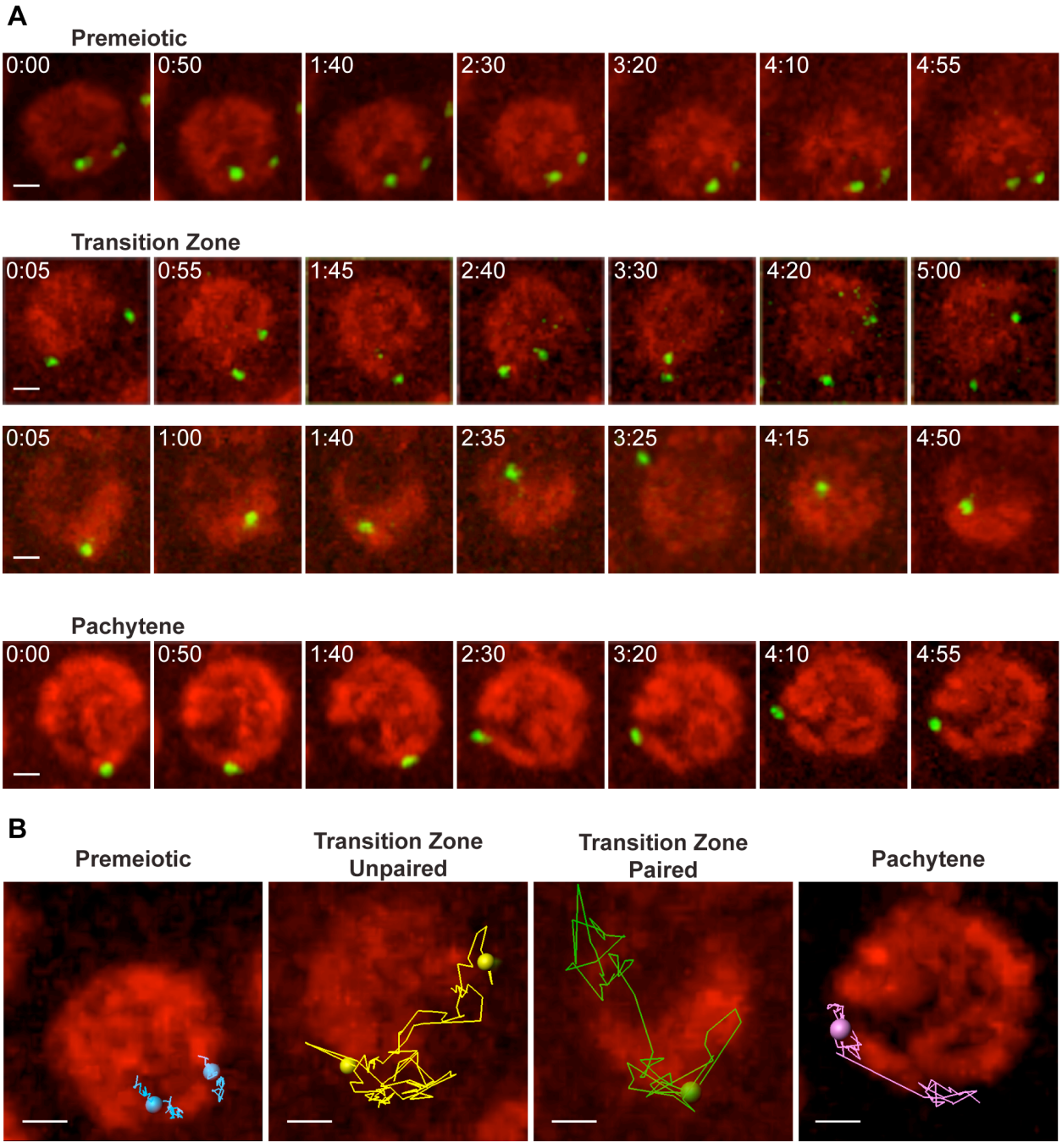

Figure 7. X chromosome Pairing Centers become extremely dynamic in meiotic nuclei.
(A) Projection images showing GFP::HIM-8 (green) and mCherry::Histone (red) from single nuclei representitive of the indicated meiotic stage. Timepoints were selected at roughly 50s intervals.
(B) Colored tracks represent all motion of the GFP::HIM-8 foci in the nuclei shown in (A) over the 5min data collection. Tracks are displayed over a single timepoint image.
Scale bars = 1 μm

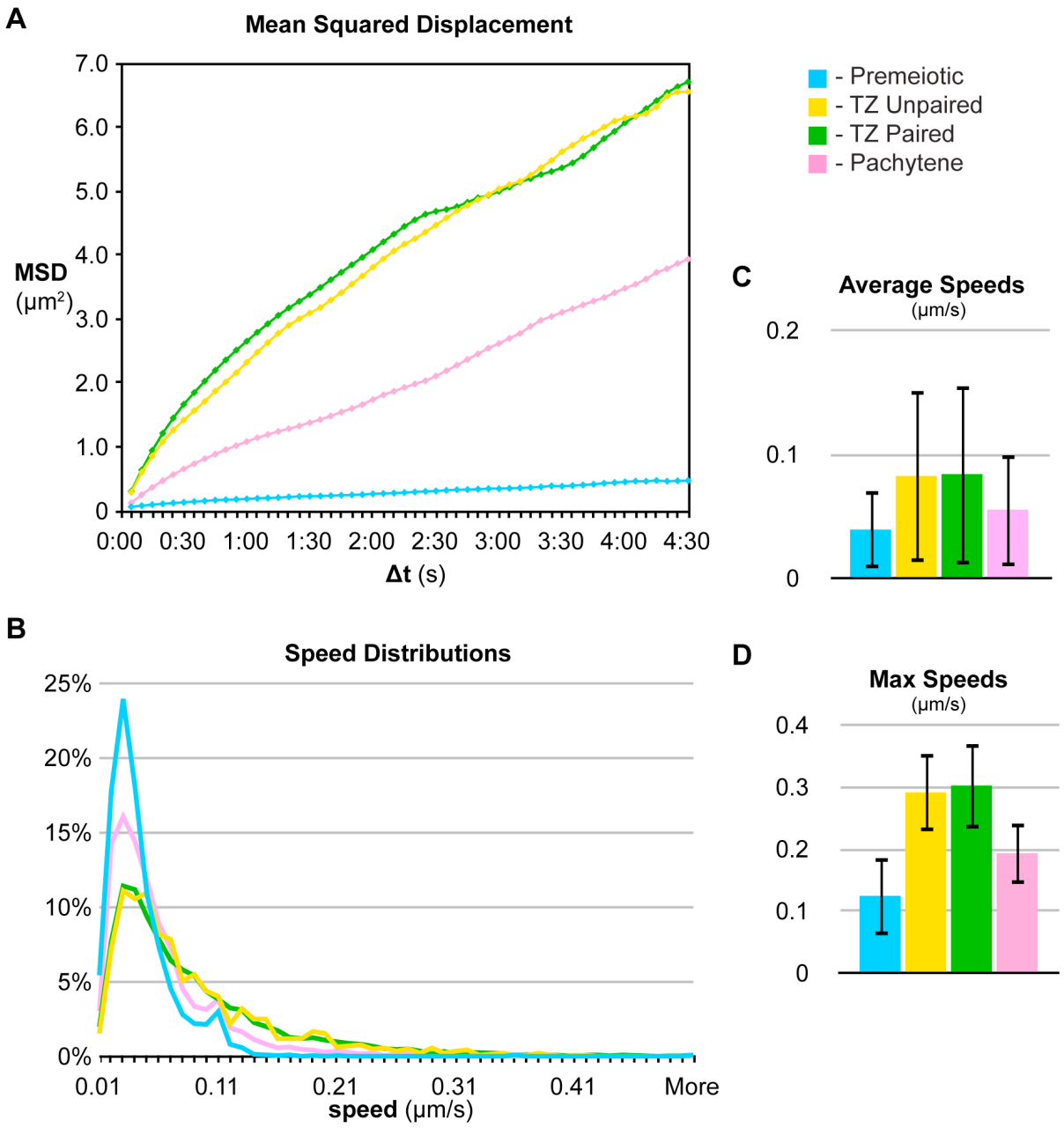

Figure 8. Occasional fast movements are responsible for large increases in the mobility of meiotic chromosomes.
(A) Mean Squared Displacements calculated for all time intervals for every trajectory (n = 38, 26, 65, 33 trajectories for Premeiotic, Unpaired Transition Zone, Paired Transition Zone, and Pachytene, respectively).
(B) Histograms showing the distribution of all speeds measured between succesive timepoints from multiple trajectories.
(C) Average speeds for all data shown in (B). Error bars indicate standard deviation.
(D) Average of the maximum 5% of speeds shown in (B). Error bars indicate standard deviation.

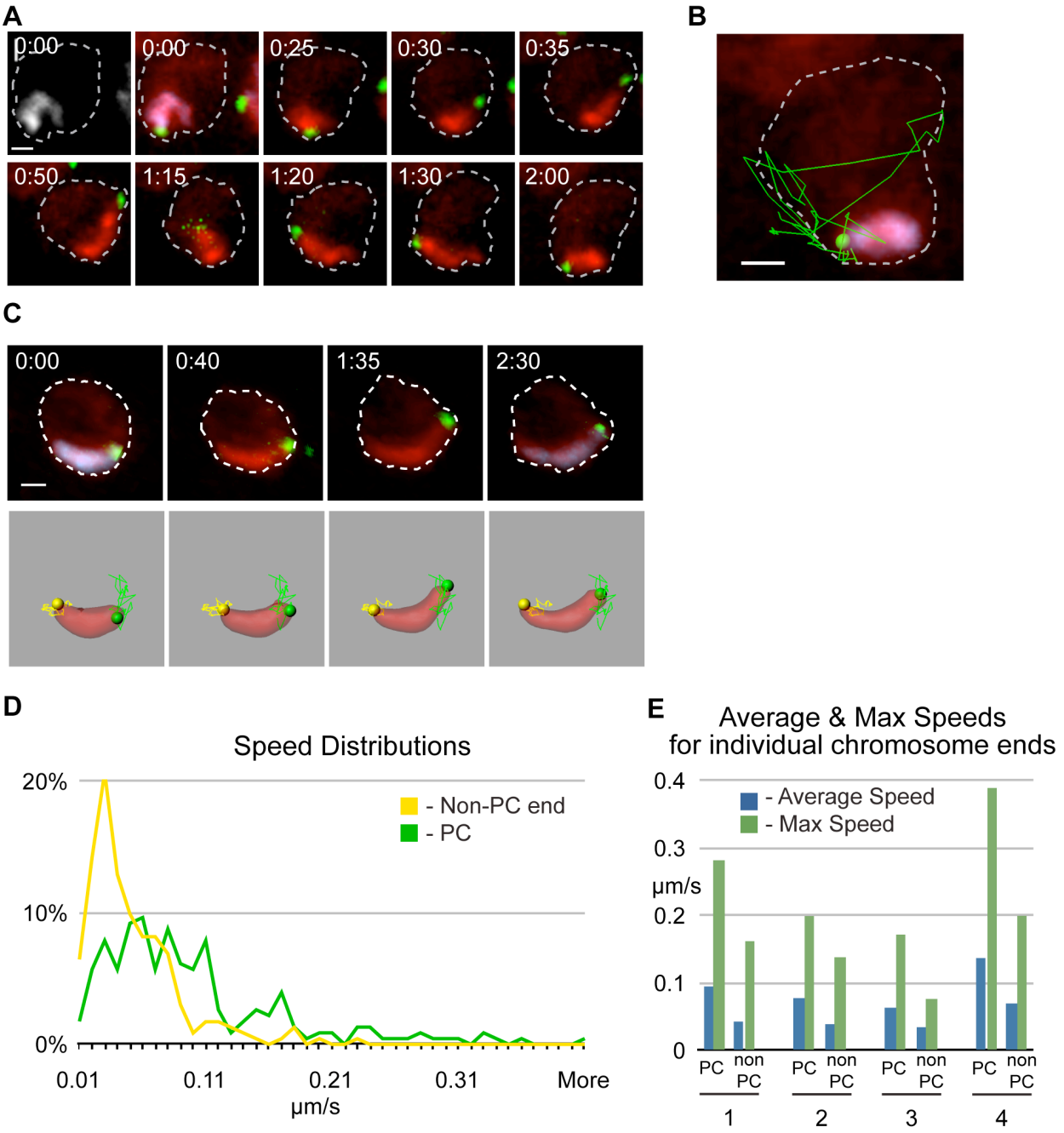

Figure 9. X chromosome motion occurs mostly at the Pairing Center end.
(A) Timelapse series of selected timepoints for a nucleus in which the X Chromosome can be visualized due to Cy5-dUTP incorporation (white in first time point, red in subsequent) along with the X PCs (green). Nuclus is outlined because mCherry::Histone signal is much more dim than that of the Cy5-dUTP.
(B) Green tracks depict all X PC motion over a 5 min data collection for the nucleus in (A)
(C) Timelapse series of a nucleus labeled as in (A) with segmentation of the X Chromosome, X PC (green) and non PC end (yellow) shown below. Tracks depict all motion over 5 min timecourse.
(D) Speed distribution for X PCs and non-PC ends for 4 nuclei segmented as shown in (C).
(E) Comparison of the average speeds and average maximum 5% of speeds between the PC and non-PC ends of single X Chromosomes. All scale bars = 1 µm.

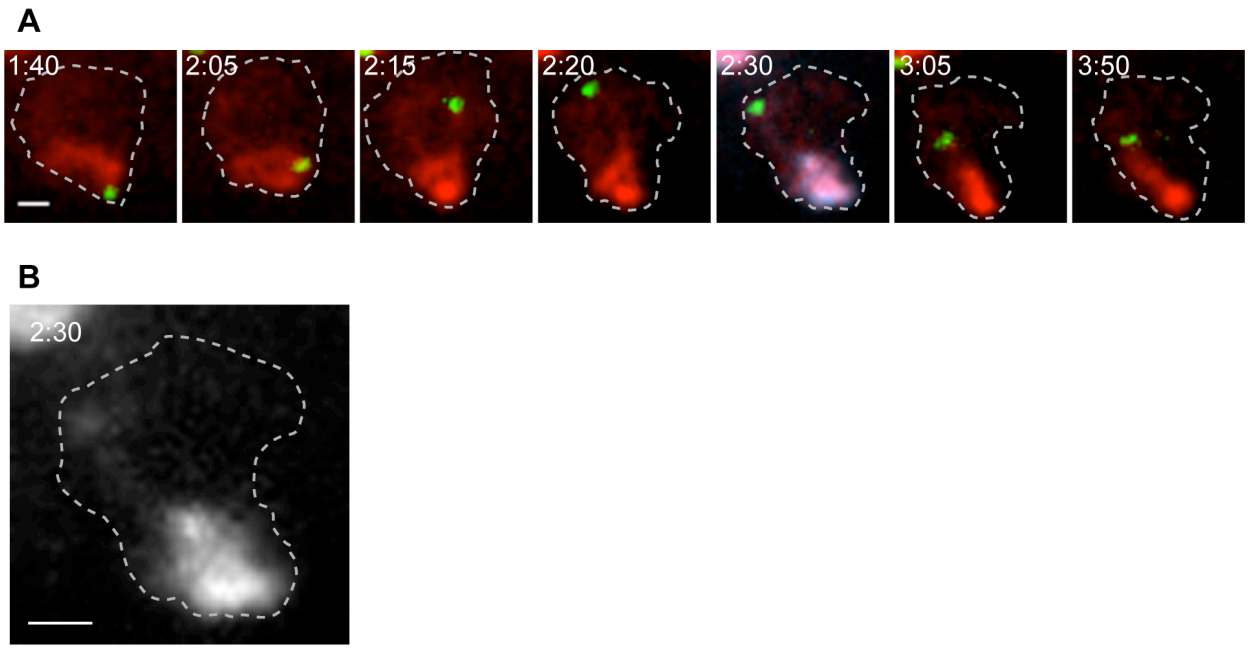

Figure 10. X chromosome imaging shows that the chromosome is elastic.
(A) Timelapse series of selected timepoints for a nucleus in which the X Chromosome can be visualized due to Cy5-dUTP incorporation (red in all timepoints and also blue at 2:30) along with the X PCs (green). Nuclus is outlined because mCherry::Histone signal is much more dim than that of the Cy5-dUTP.
(B) Cy5-dUTP signal alone (white) for the 2:30 timepoint. Faint signal can be seen extending from the bulk of X Chromosome to the site of the PC in the upper left corner (not shown).
Scale bars = 1 μm

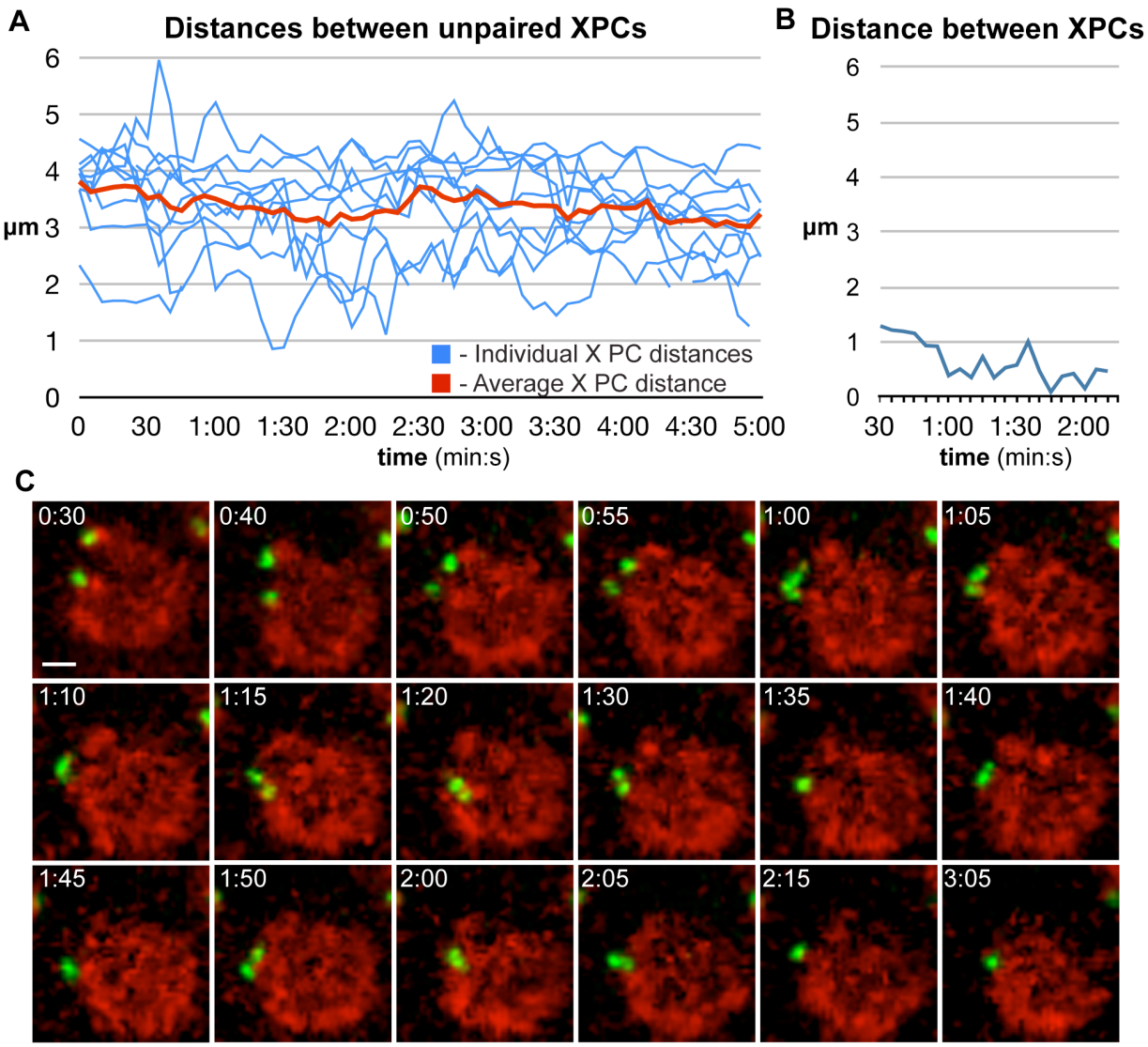

Figure 11. Capturing pairing events at the X chromosome Pairing Center is rare.
(A) Plots of the distances between X PCs in 10 nuclei (blue) and the average of these distances (red).
(B) Qantification of X PC distances for the nucleus shown in (C).
(C) Timelapse series of selected timepoints for a nucleus in which X PCs (green) pair. mCherry::Histone (red), scale bar = 1 µm.

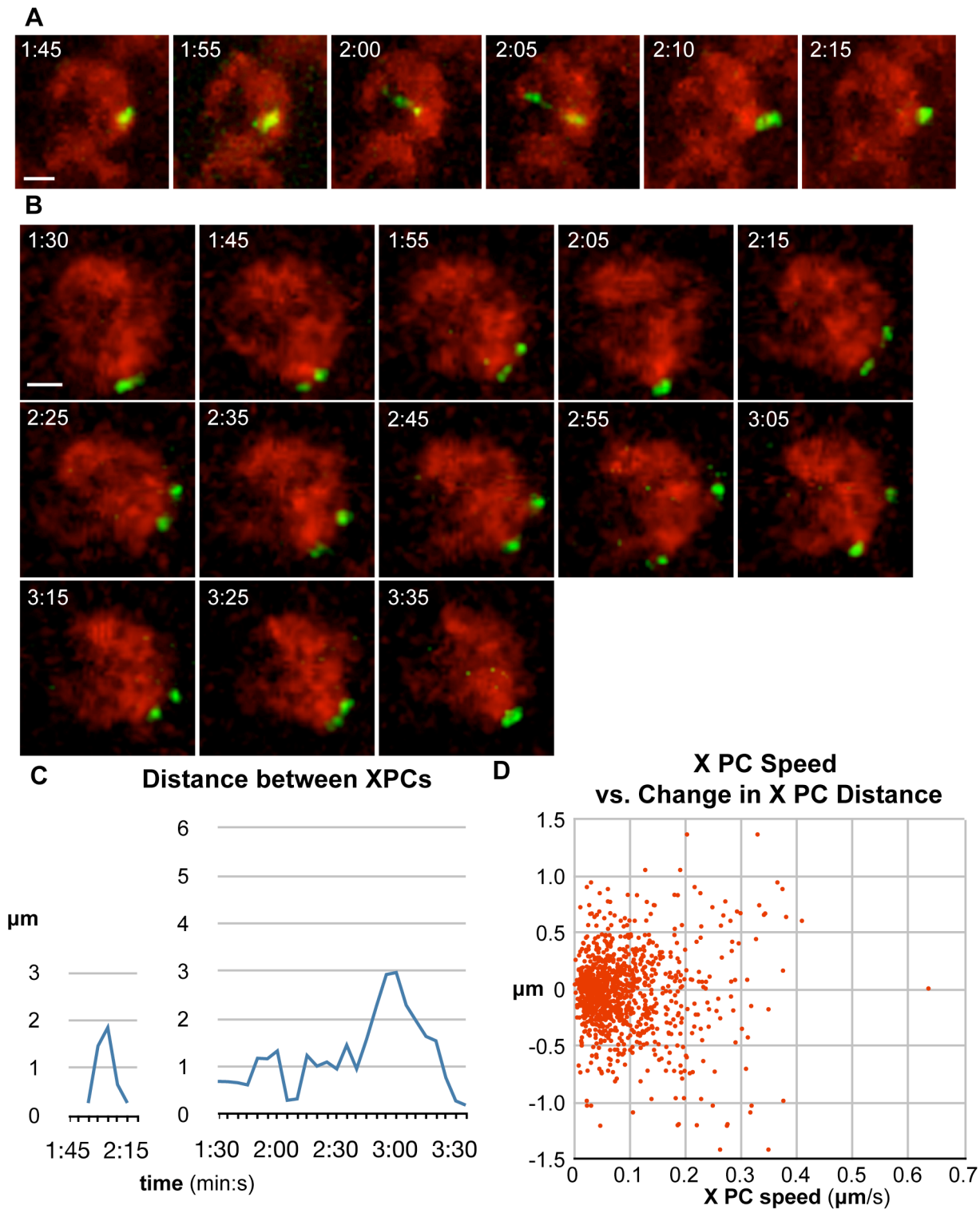

Figure 12. Paired Pairing Center loci can unpair and rapid motion does not promote pairing.
(A and B) Timelapse series of selected timepoints for a nucleus in which X PCs (green) become temporarily unpaired after having paired. mCherry::Histone (red), scale bars = 1 µm.
(C) Qantification of X PC distances for the nuclei shown in (A), left and (B), right.
(D) Plot of the change in distance between X PCs against the speed at which the PC moved in that timespan. Each point represents a 5s interval for a single X PC.

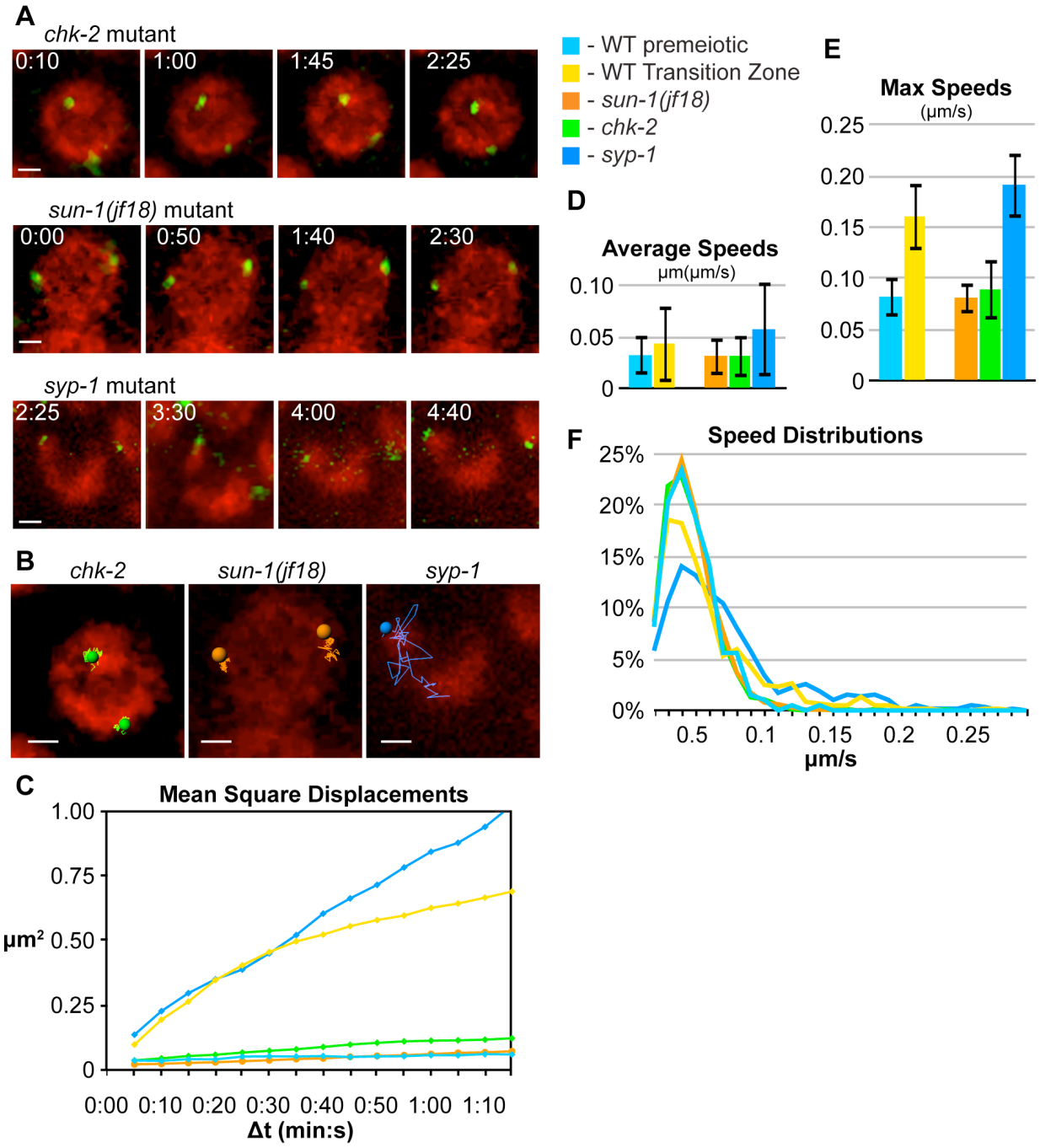

Figure 13. Rapid motion at the Pairing Center depends on the presence of meiotic nuclear envelope patches.

(A) Projection images showing GFP::HIM-8 (green) and mCherry::Histone (red) from single nuclei representitive of the indicated mutant. Timepoints were selected at roughly 50s intervals.

(B) Colored tracks show all motion of the GFP::HIM-8 foci in the nuclei shown in (A) over the 5min data collection. Tracks here were generated from projection images so quantification represents only motion in the X and Y dimensions. Scale bars = 1 µm.

(C) Mean squared displacements for all time intervals from every trajectory (n = 5, 15, 22, 40, and 15 trajectories for wildtype premeiotic, wildtype transition zone, *chk-2*, *sun-1*, and *syp-1*, respectively.

(D and E) Average and average top 5% of speeds from all tracks. Error bars show standard deviation.

(F) Histograms of all speeds recorded from 5s timeintervals.

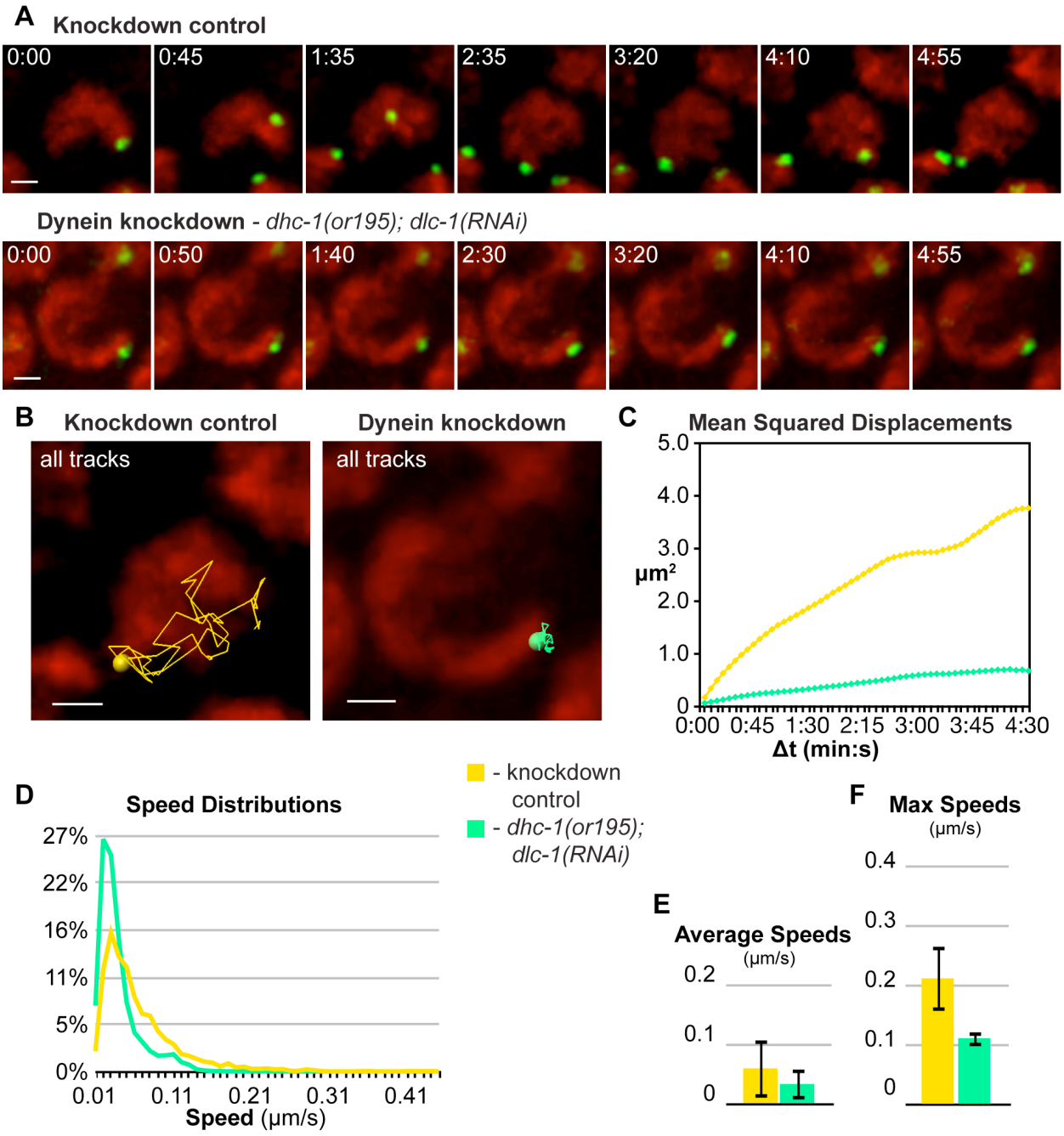

Figure 14. Rapid motion at the Pairing Center depends on dynein.
(A) Time series of projection images showing GFP::HIM-8 (green) and mCherry::Histone (red) from single nuclei representitive of dynein and control knockdowns. Timepoints were selected at roughly 50s intervals. Scale bars = 1 μm
(B) Colored tracks show all motion of the GFP::HIM-8 foci in the nuclei shown in (A) over the 5min data collection. Scale bars = 1 μm
(C) Mean Squared Displacements calculated for all time intervals for every trajectory (n = 45 trajectories for both dynein knockdown and control knockdown).
(D) Histograms of all speeds recorded from 5s time intervals.
(E and F) Average and average maximum speeds from all tracks. Error bars show standard deviation.

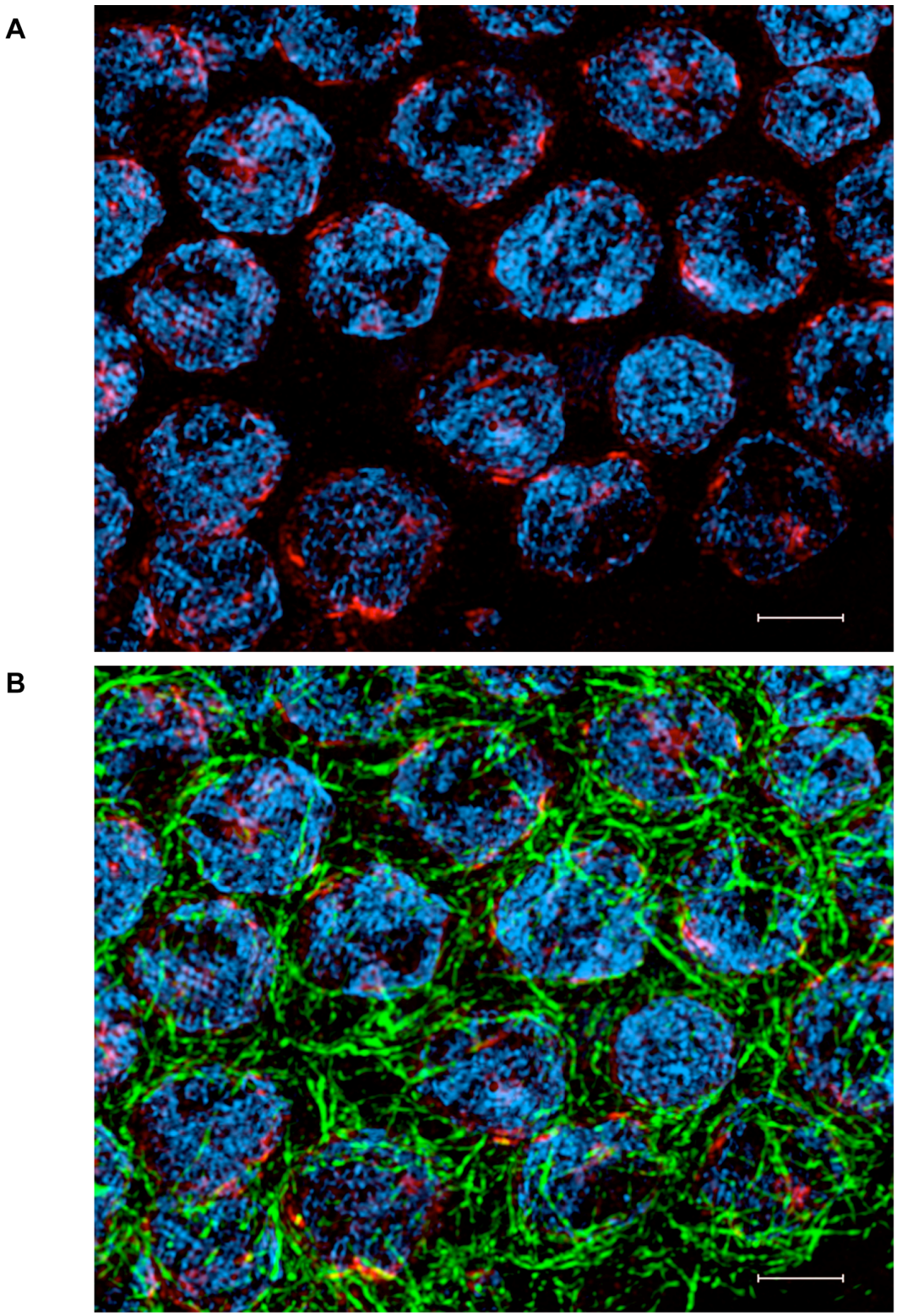

Figure 15. A dense network of microtubules surrounds meiotic nuclei and associates with a subset of ZYG-12 patches.
(A and B) Projections of meiotic nuclei stained with DAPI (blue) and antibodies recognizing ZYG-12 (red) and αTubulin (green). Scale bars = 5 μm.

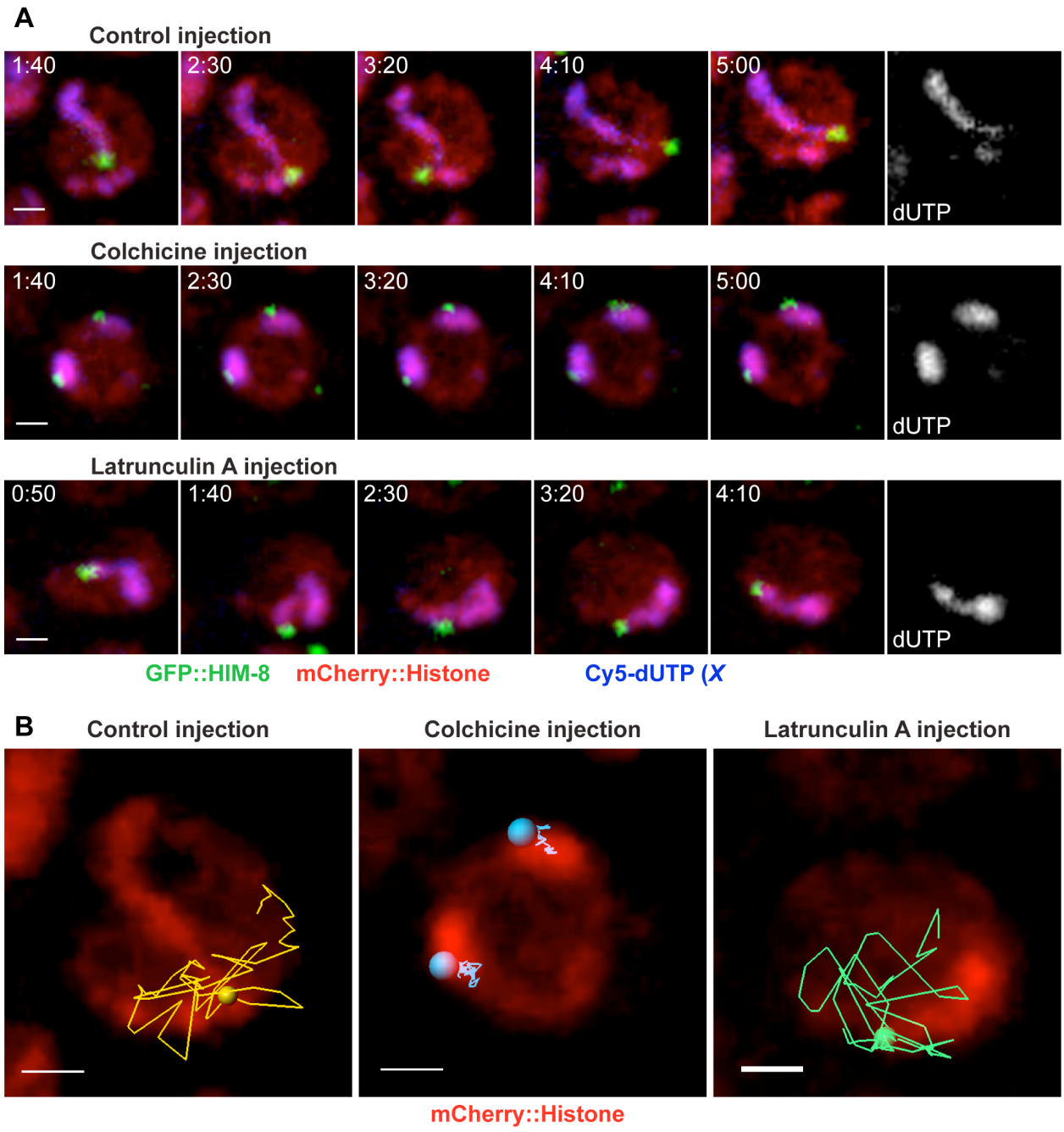

Figure 16. Rapid motion at the Pairing Center requires microtubules but is insensitive to actin depolymerizing drugs.
(A) Time series of projection images showing GFP::HIM-8 (green) and mCherry::Histone (red) and Cy5-dUTP (blue) from single nuclei representitive of the indicated treatments. Timepoints were selected at 50s intervals. Scale bars = 1 μm.
(B) Colored tracks show all motion of the GFP::HIM-8 foci in the nuclei shown in (A) over the 5min data collection. Scale bars = 1 μm.

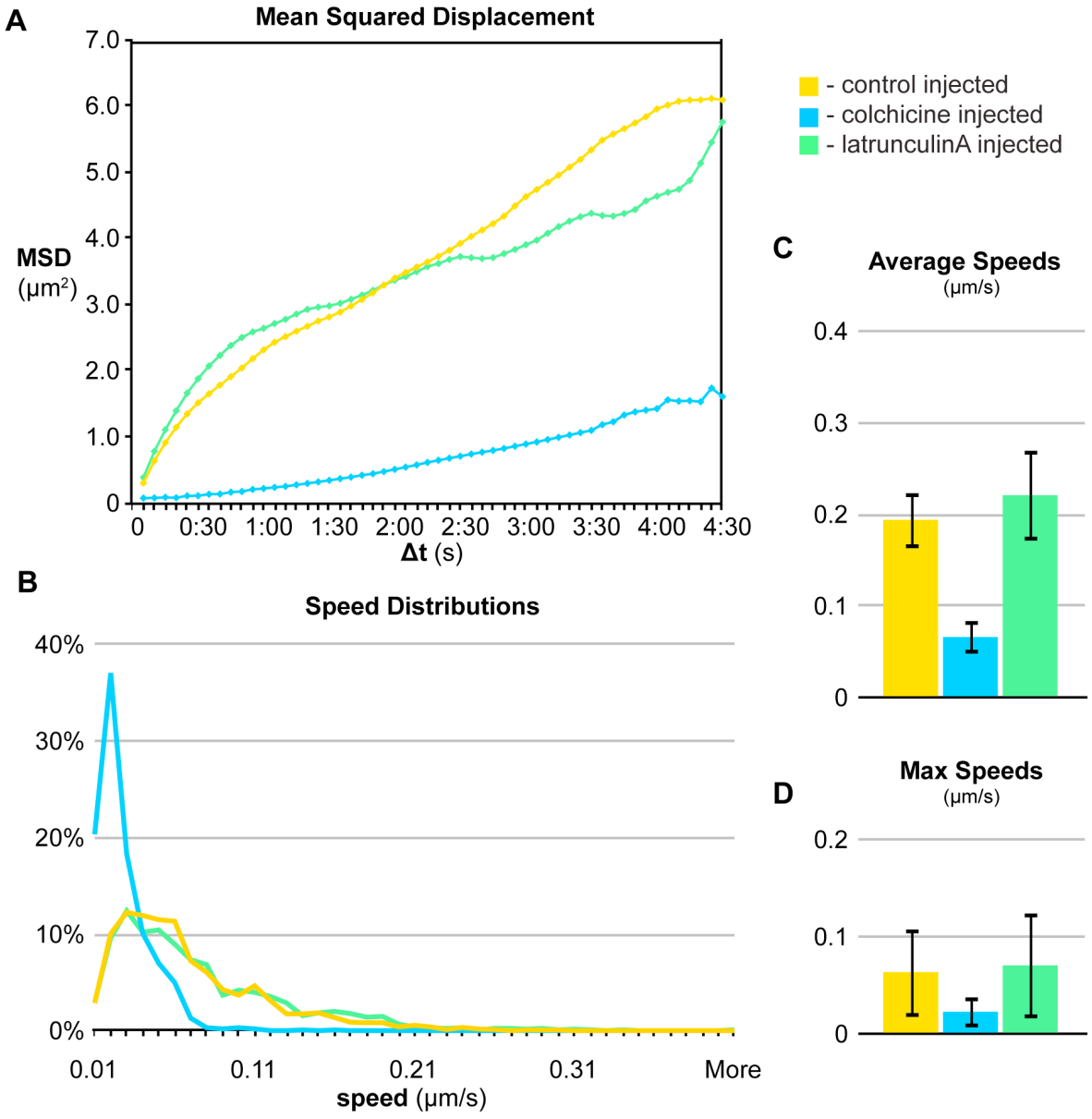

Figure 17. In the absence of microtubules, the dynamics of meiotic nuclei resemble that of premeiotic nuclei.
(A) Mean Squared Displacements calculated for all time intervals for every trajectory (n = 32, 31, and 24 trajectories for control, colchicine, and latrunculinA injected animals, respectively).
(B) Histograms of all speeds recorded from 5s time intervals.
(C and D) Average and average maximum speeds from all tracks. Error bars show standard deviation.